TRABAJO FIN DE MASTER EN

INGENIERÍA QUIMICA "PRODUCCIÓN Y CONSUMO SOSTENIBLE"

Curso: 2013 – 2014

TITULO DEL TRABAJO FIN DE MASTER

Desarrollo de materiales de membrana robustos, selectivos y de alta permeabilidad para la separación de CO_2

TITLE IN ENGLISH

Development of highly permeable, selective and robust membrane materials for CO_2 separation

AUTOR

Apellidos: Fernández Barquín

Nombre: Ana

DIRECTOR

Clara Casado Coterillo

Santander a 11 de Julio de 2014

Outline

Abstract

The ability of membranes to separate efficiently CO_2 from other light gases has received a great deal of attention due to its importance as alternative energy-efficient process reducing greenhouse gas emissions. The aim of research is to develop membrane materials that exhibit good performance and that are robust enough for long-term operations at the process temperatures. The permeability and selectivity values of membranes should be as high as possible for their efficient use in industrial gas separation applications. Poly (1-trimethylsilyl-1-propyne) (PTMSP) has the highest known permeability of any polymer to gases. However, the high permeability is coupled with low ideal selectivity and its gas permeability decreases rather dramatically with time because of physical aging. Many attempts have been made to overcome this problem: crosslinking, substitution of functional groups, mixed matrix membranes.

Mixed-matrix membranes (MMMs) exhibit the molecular sieving effect and catalytic properties of inorganic fillers and combine desirable mechanical properties with the economical processing capacity of polymers. The main challenge of MMMs is the adhesion between the zeolites and the polymer to obtain a good interaction. Numerous attempts have been reported to incorporate zeolite particles into polymer matrices for gas separation because of their crystalline character with well-defined pore structures and shape selectivity properties.

In this work, mixed matrix membranes have been prepared from PTMSP and small pore zeolites, such as NaA (Si/Al =1) and ITQ-29 (Si/Al = ∞), at different loadings, and the CO_2 and N_2 permeation has been measured at temperatures from 25 to 100ºC. The physical aging of the PTMSP is delayed. The permeability and selectivity increase with increasing zeolite A loading, up to an optimum zeolite loading of 10 wt.%. Maxwell model has been used to predict MMMs performance but the predicted values underestimate the experimental results. TGA and XRD reveal that the MMMs are thermally stable up to 300ºC and there is good interaction between zeolites and polymer.

Keywords: Mixed-matrix membranes, Zeolites, Gas separation, Poly (1-trimethylsilyl-1-propyne), Permeability. Thermal stability.

1. Introduction

Global carbon emissions from fossil fuels have significantly increased since 1900. Emissions increased by over 16 times between 1900 and 2008 and by about 1.5 times between 1990 and 2008. The recently released IPCC 4th Assessment Report confirmed that warming of the global climate system is unequivocal, and that anthropogenic greenhouse gas (GHC) emissions are very likely (>90% probability) the cause [1].

Carbon dioxide emissions from fossil fuel combustion are a major contributor to climate change. One step toward reducing CO_2 emissions is to capture the CO_2 generated during combustion and store it in a suitable place. This process of carbon capture and storage (CCS) has the potential to reduce future world emissions from energy by 20% [2]. The conventional technology applied for carbon capture is chemical absorption in a liquid solvent. However, numerous challenges remain for this type of application, such as too high energy requirement, solvent losses by flooding, amine deactivation or secondary CO2 production associated to solvent regeneration by steam [3].

The ability of membranes to separate efficiently CO_2 from other light gases has received a great deal of attention due to its importance as alternative energy-efficient process reducing greenhouse gas emissions [4]. A number of advantages, such as low operating and capital costs, lower energy requirements, ease of operation and ease of scale up are offered by membrane separation.

Membrane materials should present good performance and be robust enough for long term operations. Besides, they have to present high permeability values and well as good selectivity values for their utility in industrial gas separation applications.

Generally, durability, mechanical integrity at the operating conditions, productivity and separation efficiency are criteria for selecting membrane materials. The commercially available membranes for gas separation are polymeric, which have limitations working at elevated temperatures or with high presence of water. Inorganic membranes, such as zeolite membranes, have been studying during last decades due to zeolite capacity to discriminate between small molecules and resist operation conditions that organic membranes are not able to. However, due to the manufacturing difficulty, reproducibility and cost, commercial inorganic membranes for gas separation are not yet available [5].

Polymer membranes are the most advance choice for membrane technology CO_2 separation processes. Polymeric membranes working at temperatures of up to 200°C are candidates for post-combustion processes. There are different commercial polymeric membranes for CO_2 capture made of different materials (Table 1).

Table 1. Commercial polymeric membranes for CO_2 capture [6]

Membrane (Supplier)	Supplier	Membrane material
Polyactive ®	GKSS (Germany)	Silicone rubber
PDMS 4060	(Sulzer (Germany)	Polydimethylsiloxane
Separex	UOP (USA)	Cellulose acetate
Polaris ®	MTR (USA)	Silicone rubber

Their main advantages are that are already commercially available, low cost and easy reproducibility. The main drawbacks are the thermal, mechanical and chemical resistance, the problems with the water vapor and the CO_2 plasticization.

The gas separation polymeric membranes traditionally show a trade-off on their permeability and selectivity for a specific gas-pair mixture separation [7]. High selectivity and permeability lead into a smaller membrane area and lower driving force to achieve a given separation; therefore, a more efficient separation process [8]. Glassy polymer membranes are better thermal stability and mechanical properties. Rubbery polymer membranes show higher permeability but low selectivity.

Poly (1-trimethylsilyl-1-propyne) (PTMSP) has garnered much interest in the last 20 years because it has the highest known permeability of any polymer to gases and vapors. Its high permeability is based on high solubility and high diffusivity and is probably related to its extremely large free volume (0.29) and a very low density (0.75 g/cm^3), relative to that of other polymers [9]. This accounts for the low chain mobility with glass transition temperature greater than 250ºC, and glassy nature, that exhibits poor packing in the solid state. This is attributed to the presence of alternating double bonds in the backbone and a bulky trimethylsilyl [$Si(CH_3)_3$] side group [10].

The large amount of “open” space in the PTMSP matrix makes it a very poor molecular sieve, and consequently differences in solubility from penetrant to penetrant are usually greater than differences in diffusion coefficients. The permeability of permanent gases in PTMSP increases as temperature is reduced, which is opposite to

the behavior of most other glassy polymeric membranes and even rubbery polymer poly(dimethylsiloxane) (PDMS) [11].

The gas permeability of PTMSP decreases rather dramatically with time due to physical aging leading to relaxation of the enormous levels of excess free volume or due to oxidation of the double bonds in the chain backbone [12]. Many efforts have been directed to improve this for obtaining robust and durable membranes: crosslinking [13], substitution of functional groups [9], mixed matrix membranes [14].

The high permeability of PTMSP is coupled with low ideal selectivity (the ratio of the single gas permeabilities of two permeants).

Mixed-matrix membranes (MMMs) exhibit the molecular sieving effect and catalytic properties of inorganic fillers and combine desirable mechanical properties with the economical processing capacity of polymers [8,15][15].

Material selection for both matrix and sieve phases is a key aspect in the development of mixed matrix membranes. Polymer matrix selection determines minimum membrane performance, and the addition of properly selected molecular sieves can only improve membrane selectivity in the absence of defects [16]. The choice of an inorganic phase as fillers in MMMs suitable for the separation process is of great significance. Typical inorganic fillers are zeolites, activated carbons, carbon molecular sieves, non-porous silica and graphite [8]. Numerous attempts have been reported to incorporate inorganic particles into PTMSP matrices for gas separation [11,17]. A significant effort has been devoted to prepare membranes using zeolites as filler due to their size and shape selective properties and glassy polymers as the polymer matrix due to their rigidities and higher intrinsic selectivities [18]. Despite their crystalline character with well-defined pore structures and shape selectivity properties, providing high thermal, mechanical and chemical stability, only one work has been reported so far to improve butane permselectivity of PTMSP membranes by porous zeolites [14].

Zeolites are porous crystalline alumina-silicates composed of AlO_4 and SiO_2 tetrahedra, and the Si/Al ratio can be varied to incorporate elements that differ from both the aluminum and silicon. The adsorption capacity of zeolites is due to their regular and stable porous structure and to the Si/Al ratio. LTA type zeolites have pore dimensions of 0.4 nm, being able to discriminate between molecules as O_2 and N_2, is used in air separation.

The zeolite uptake of CO_2 is strongly influenced by framework structure and composition, as well as the location and composition of extra-frameworks cations. LTA type zeolites have been shown to have good working capacities that can be modified according to the chosen process conditions [19].

Most of the studies on NaA zeolite membranes are focused on the dehydration of organic solutions [20] and only few gas permeation studies are reported [5].

In this work, zeolite A frameworks with different Si/Al ratio were selected to improve the PTMSP separation performance in CO_2/N_2 separation, because of its small pore (0.4 nm). CO_2/N_2 gas separation performance has been evaluated, taking into account the influence of temperature in the process and the materials stability. Membranes have been also characterized by SEM, TGA-DTA, XRD, adsorption and permeation of CO_2 and N_2.

2. Experimental

2.1 Membrane preparation

Polymer and mixed matrix membranes were prepared by the solution casting method. In a typical synthesis:

Poly (1-trimethylsilyl-1-propyne) (PTMSP, Gelest) was dissolved in toluene to make a 1.5 wt% polymer solution. Prior to preparing the sample solution, PTMSP, Gelest was dried in an oven at 60ºC to eliminate possible humidity. The mixture was dissolved after 24 h by refluxing in an oil bath at 60ºC. After that, the solution was filter by a filter system with a vacuum pump to eliminate possible impurities. The casting volume was sonicated for 10 minutes for degassing. Dense films were prepared by casting 10 mL onto a glass plate. The films were allowed to dry for 2 – 3 weeks covered with a Petri dish to evaporate the solvent at ambient conditions. Removal of the film from the glass substrate was carried out by washing with copious amounts of deionized water. Some films were measured as-made, other films were stored in liquid methanol and dried before gas permeation experiment, and others immersed in methanol for 5 min prior to the measurements, in order to prevent physical aging.

The membrane thickness was carefully measured using a digital micrometer (Mitutoyo digimatic micrometer, IP 65) with a precision up to 0.001 mm. Five points of the membrane effective area are measured and the average thickness and standard deviations were calculated therefrom.

The dry weight of the membranes was also measured before experiment and, for selected samples of each composition, also after the permeation set of experimental runs, in order to monitor changes in density that could reveal physical aging and other phenomena in the membrane material.

2.2 Gas permeation measurements

The pure gas permeability was measured using the experimental set up in Fig. It consists of a membrane module, connected, by means of a series of pneumatic controlled valves, to the feed and permeate sides. A punctual and a differential transducer (Omega, UK) measure the pressure level in the feed side and in both membrane sides during the whole experiment, in order to monitor the gas volume which goes through it. The membrane module is placed in a convection oven (Memmert, Germany). The permeation cell is composed by two parts pneumatically pressed each

other on a Viton ring that seals the membrane. Basically the membrane is placed over a stainless steel permeation cell leading to an effective area about 14.05 cm^2.

Gas permeation tests were carried out in a temperature range of 25 – 100 ºC, feeding the single gases at 2 – 3 bar and evacuating the permeate to generate the pressure difference. The gases have been tested in the following order: N_2 and CO_2, evacuating both the feed and the permeate side before each measurement Before each measure the air tightness of the system has been checked.The same protocol has been followed for pure polymer and mixed matrix membranes.

Time-lag method has been used to estimate the diffusion coefficient through the membranes, according to the equation (1).

$$D=\delta^2/6\theta \quad (1)$$

Where δ is the membrane thickness and θ is the time lag obtained extrapolating to the time axis the linear part of the experimental curve in the accumulated permeate volume vs. time plot [21]. In this work, the time lag has been used to calculate the steady-stable permeation flux after the time-lag. The diffusivity values obtained experimentally this way are orientative.

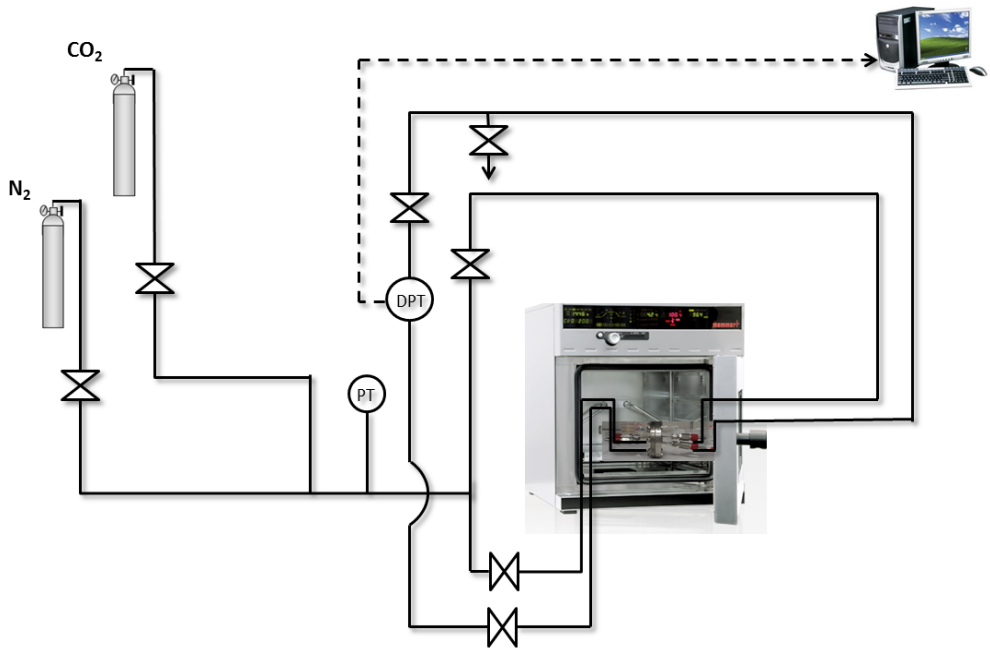

Figure 1. Experimental setup for gas permeation measurements

The gas permeation throw dense polymeric membranes is described by adsorption of the gas onto the membrane material, diffusion across the membrane and desorption in

the permeate side. Both the adsorption and desorption steps can be described by the Henry's law (Equation (2)).

$$C_i = S \cdot p_i \tag{2}$$

Where C_i is the gas concentration in the membrane surface, p_i is the gas partial pressure and S_i is describes the solubility of the gas in the membrane material, and exhibits van't Hoff temperature dependence (Equation (3)).

$$S_i = S_{i,0} \cdot e^{-\frac{\Delta H_{S,i}}{R \cdot T}} \tag{3}$$

The diffusion step is described by the Fick's law (Equation (4)):

$$J_i = -D_i \frac{dC_i}{dx} \tag{4}$$

Where J_i is the flux of the gas through the membrane ($mol \cdot m^{-2} \cdot s^{-1}$), C_i is the gas concentration ($mol \cdot m^{-3}$), and D_i is the diffusivity coefficient of the gas i in the membrane material ($m^2 \cdot s^{-1}$), which exhibits the same temperature dependence as the Henry's constant due to its thermal character (Equation (5)).

$$D_i = D_{i,0} \cdot e^{-\frac{\Delta H_{D,i}}{R \cdot T}} \tag{5}$$

Combining the previous equations, the following expression is achieved and describes the transport of a component through a dense membrane and applying a mass balance to the membrane material, equation (6) is achieved.

$$J_i = -D_i \cdot S_i \frac{(p_{i,f} - p_{i,p})}{\delta} = -P_i \frac{(p_{i,f} - p_{i,p})}{\delta} \tag{6}$$

Applying a mass balance to the membrane material, the following equation is achieved, where P_i is the permeability constant, δ is the membrane thickness, $p_{i,f}$ is the partial pressure of the gas i in the feed side and $p_{i,p}$ is the partial pressure of the gas i in the permeate side.

As a result, the permeation of a gas through a polymer-based membrane is usually described by the solution-diffusion model (Equation (7)):

$$P = D \cdot S \tag{7}$$

The permeability represents the amount of molecules that cross the membrane and is described by the equation (7), where D is de diffusion coefficient and S the solubility

coefficient. Diffusivity (D) is the measure of the amount of mobility of the molecules passing through the voids of the polymer. The solubility (S) is related to the number of dissolved molecules in the polymer. Thus the permeability is given by the product of the diffusion coefficient, a kinetic factor, and the solubility coefficient, a thermodynamic factor, both being influenced by temperature.

The pure gas permeability was calculated from the feed and permeate pressures by the equation (8) [22].

$$ln\left|\frac{\left(p_{i,f}-p_{i,p}\right)_0}{\left(p_{i,f}-p_{i,p}\right)}\right| = ln\left|\frac{\Delta P_0}{\Delta P}\right| = \left(\frac{P}{\delta}\right)\beta_m t \quad (8)$$

where β_m is a geometric factor describing the feed and permeate volume spaces and $p_{i,f}$ and $p_{i,p}$ are the pressures in the feed and the permeate compartment respectively, the time and δ is the membrane thickness. Thus, when Ln ($\Delta P_0/\Delta P$) is represented versus time, the slope gives as the permeability in m^2/s. Permeability is often reported in units of barrer, which is defined as:

$$1\ Barrer = 10^{-10}\frac{cm^3(STP)\ gas \cdot cm\ thickness}{cm^2\ membrane\ \cdot s\ \cdot cmHg}$$

The selectivities were calculated as the ratio of the corresponding permeabilities of two pure different gases.

The ideal selectivity is the ability to separate two molecules of a mixture (eg, CO_2 and N_2, in this work) thus it is an intrinsic property of the membrane material, which can be calculated from the ratio of the pure gas permeabilities, defined by the equation (9).

$$\alpha = \frac{P_{CO_2}}{P_{N_2}} \quad (9)$$

Therefore, the difference between permeabilities of different gases through the membrane is not due just to the diffusivity, but also influenced by the physicochemical interactions of these gases with the membrane material, which determines the amount of gas flowing per unit volume (S). Membranes should present both high permeability and selectivity, because a high permeability will make necessary a smaller membrane area, while a high selectivity provides a greater purity of gas at the exit.

MMM material performance can be predicted using various theoretical expressions but Maxwell's, which was originally derived for the estimation of the dielectric

properties, has been widely accepted as an easy and effective tool for estimating MMM properties [8,23].

According to the Maxwell model, the overall steady-state composite permeability is given by the equation (10).

$$P_{eff} = P_c \cdot \frac{P_d + 2P_c - 2\emptyset(P_c - P_d)}{P_d + 2P_c + \emptyset(P_c - P_d)} \quad (10)$$

Where P_{eff} is the effective composite membrane permeability, $\emptyset$ the volume fraction, P the single component permeability and the subscripts d and c refer to the dispersed and continuous phases, respectively.

2.3 Thermal Gravimetric Analysis

Thermal resistance of the samples was studied by thermo gravimetric analyses (DTA-TGA). These analyses were performed using a thermo balance (DTG-60H, SHIMADZU, Japan) in air at heating rate of 10ºC/min up to 700ºC. Samples of approximately 2 – 5 mg were loaded into an alumina crucible and a reference pan was left empty during the experiment.

2.4 CO_2 solubility experiments

CO_2 sorption experiments were carried out gravimetrically in the DTG-60H thermobalance, at a feed pressure of 5 bar and a gas flow rate around 50 mL/min at a fixed temperature, for 3 hours. The temperature range was varied from 25 to 100ºC.

2.4 X-ray diffraction analysis

The crystalline structure of the samples was investigated by means of room temperature X-ray powder diffraction (XRD). The patterns were collected on a Philips X'Pert PRO MPD diffractometer operating at 45 kV and 40 mA, equipped with a germanium Johansson monochromator that provides Cu Kα1 radiation (λ = 1.5406 Å), and a PIXcel solid angle detector, at a step of 0.05º.

2.5 Scanning Electron Microscopy

The morphology and cross-sectional areas of selected membranes are being observed by scanning electron microscopy, using a JEOL JSM 5600 equipment, at the Universidad Politécnica de Valencia. Membrane samples were immersed in liquid nitrogen and fracture and sputtered with gold before observation.

3. Results and discussion

To investigate the gas permeation properties of the membranes prepared, a set of permeation experiments have been carried out using the experimental set up described in section 2.

In Table 2 the CO_2 permeability coefficients and the CO_2/N_2 selectivity values of pure PTMSP membranes are reported as function of temperature up to 90ºC. The CO_2 permeability tends to decrease when the temperature rises, which is opposite to the behavior of most other glassy polymeric membranes and even rubbery polymers [24]. These results are in good agreement with others reported in literature [10,11,25]. A decrease in gas permeability is observed as a result of the temperature decrement. The logarithm of the permeability follows a linear relationship with the inverse of the temperature as shown in Figure 11; therefore, the temperature influence on the gas permeability is well described in terms of an Arrhenius type relationship by equation (10). The increase of temperature does not affect the CO_2/N_2 gas pair selectivity. Besides, these values of selectivity are very low, due to the trade-off between permeability and selectivity.

$$P = P_0 exp\left(-{}^{E_p}/_{RT}\right) \tag{10}$$

Where P_0 is the pre-exponential factor, Ep the activation energy of permeation, R is the gas constant, and T is the absolute temperature.

Table 2. CO_2 permeability and CO_2/N_2 selectivity values for pure PTMSP membranes

T (ºC)	P CO_2 (barrer)	α CO_2/N_2
25	17454 ± 5102	1.22 ± 0.07
30	13420 ± 2228	0.76 ± 0.2
40	13068 ± 2077	0.82 ± 0.19
50	12236 ± 2607	0.95 ± 0.06
60	12056 ± 2375	1.12 ± 0.07
70	10453	1.14
90	7779	0.98

The permeability vs selectivity values of the different membranes have been represented in the Robeson's plot (Figure 2). Regarding ZA-PTMSP membranes, it can be observed that the more filler concentration, the closer are the values to the upperbound, being overcome when the filler concentration is 10 and 20 wt%. The selectivity of these MMMs is much higher than pure polymer membranes due to the molecular sieving effect imparted by the introduction of the small-pore zeolite and the good interaction between polymer and zeolite in the membrane matrix. Besides permeabilities are not reduced, overcoming existing polymer materials performance, in spite of the fact that most MMMs were reported to suffer from poor interaction between zeolite particles and polymer chains, which caused non-selective voids at the polymer-zeolite interface and were the reason for insufficient improvement of membrane performance [18]. However, in ITQ-29-PTMSP membranes the best selectivity is achieved when the loading of the zeolite is only 5 wt%, and the permeability values decrease compared with the pure polymer (Figure 2). This could be attributed to the different Si/Al composition of ZA and ITQ-29, which may affect the interaction with the solvent upon mixing and with the polymer chains.

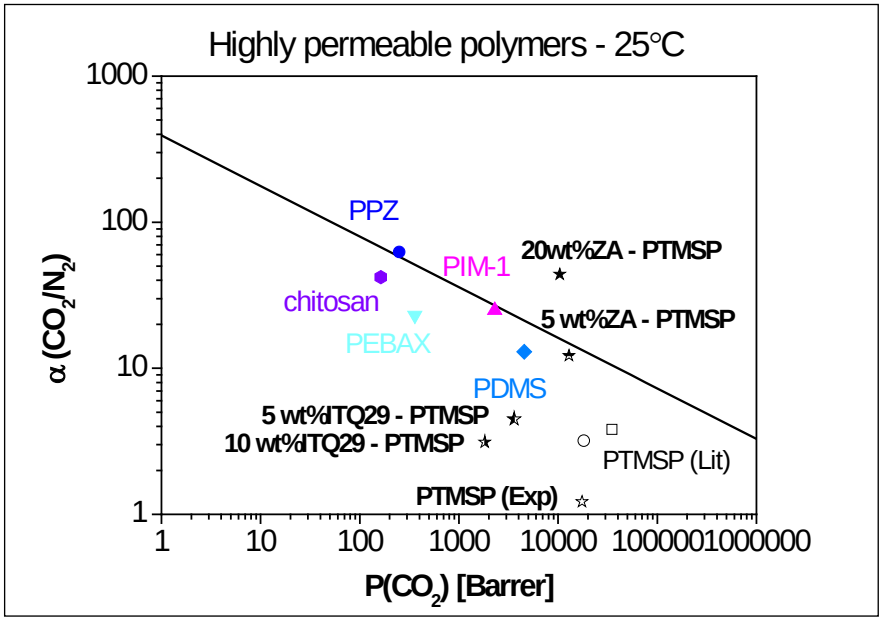

Figure 2. Robeson's upperbound.

From the X-ray diffraction (XRD) patterns of the membranes presented in Figure 3, a good interaction between the zeolite and the polymer matrix is discerned. The characteristic reflections of zeolite A become stronger upon loading increase, thus revealing their presence into the MMM matrix.

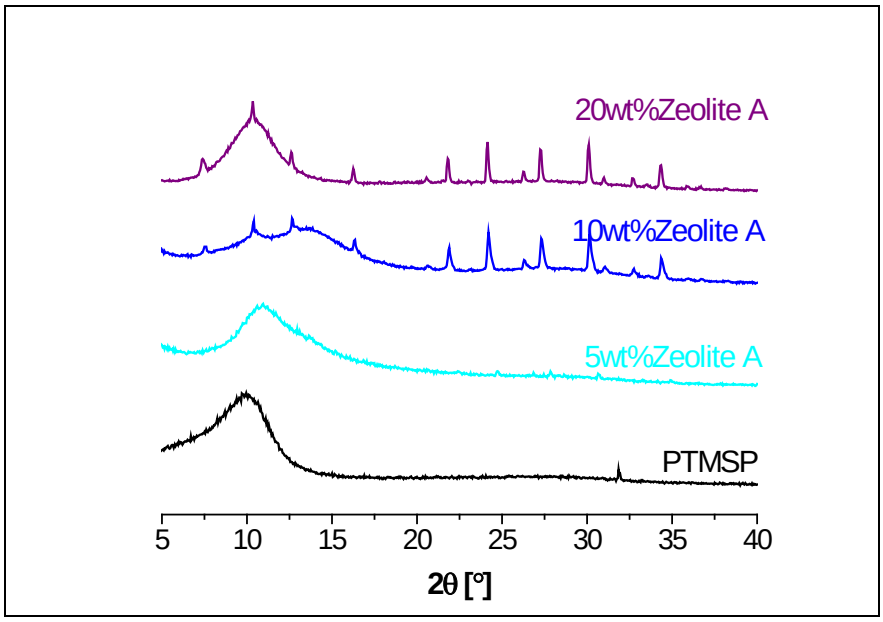

Figure 3. X-ray diffractograms of the membranes.

Thermogravimetric analyses (TGA) of the membranes are presented in Figure 4 and Figure 5. In the case of the membranes, thermal degradation starts at 300ºC and weight loss is small up to 350ºC, and the shape of the curves was very similar to that of the pure polymer because of the low zeolite/polymer concentration ratio.

The real loading of the zeolite has been calculated from the TGA analyses and for 5 wt.% ZA-PTMSP membrane is 6.8 wt.% for, the 10 wt.% ZA-PTMSP membrane 14.3%, and for 20 wt% ZA-PTMSP membrane 18.7%. In the case of ITQ-29 membranes, the real loading of zeolite is 15.8 wt.% for 10 wt.% ITQ29-PTMSP membrane and 33.5 wt.% for 20 wt.% ITQ29-PTMSP membrane.

The real zeolite loading of the membranes agreed with nominal value and the thermal stability of the membranes is similar to the glassy polymer PTMSP. The thermogravimetric experimental results indicate that the PTMSP MMMs are thermally stable in high temperature processes up to 300 ºC, which accounts for the potentiality of these membrane materials as high temperature membranes.

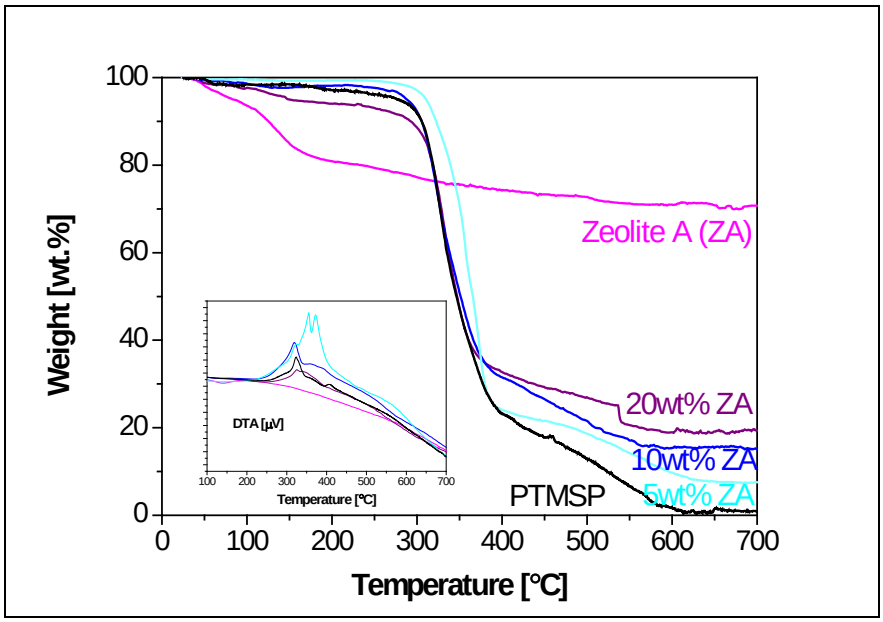

Figure 4. Thermogravimetric analyses of ZA-PTMSP membranes

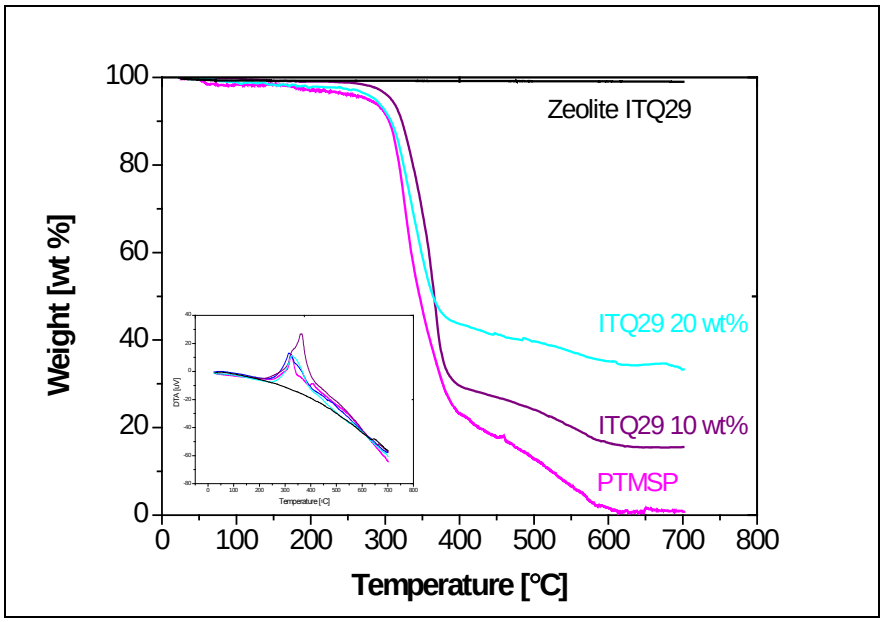

Figure 5. Thermogravimetric analyses of ITQ29-PTMSP membranes

CO_2 adsorption isotherms were conducted at 25ºC, 30ºC, 40ºC and 50ºC and 5 bar for all types of the prepared membranes. In Figure 6 and Figure 7 are represented the CO_2 adsorption isotherms for pure PTMSP and ZA-PTMSP membranes respectively and in Figure 8 for ITQ29-PTMSP membranes.

In the case of pure PTMSP membranes, the CO_2 solubility decreases with temperature, as well as the permeability does.

Regarding the MMMs, for the 5 wt.%, 10 wt.% ZA-PTMSP membranes and 20 wt.% ITQ29-membranes, their performance present a similar trend as the pure PTMSP membranes, decreasing the CO_2 adsorption with temperature, as it's usual in mixed matrix membranes. However, the CO_2 solubility increases with temperature in the case of 20 wt.% ZA-PTMSP membranes, which may be attributed to the appearance of voids between particles or the polymers and leading to different transport mechanisms.

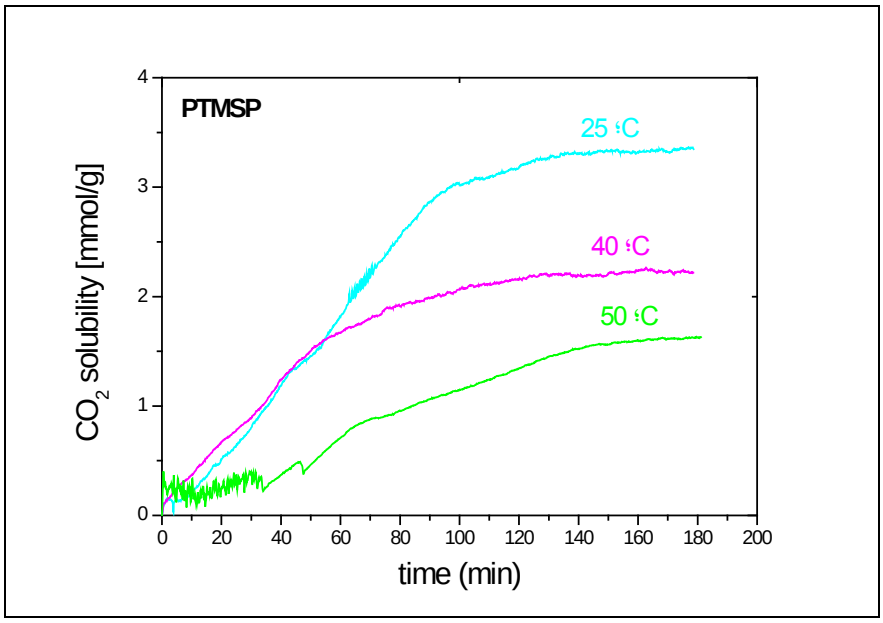

Figure 6. CO_2 adsorption curves for pure PTMSP

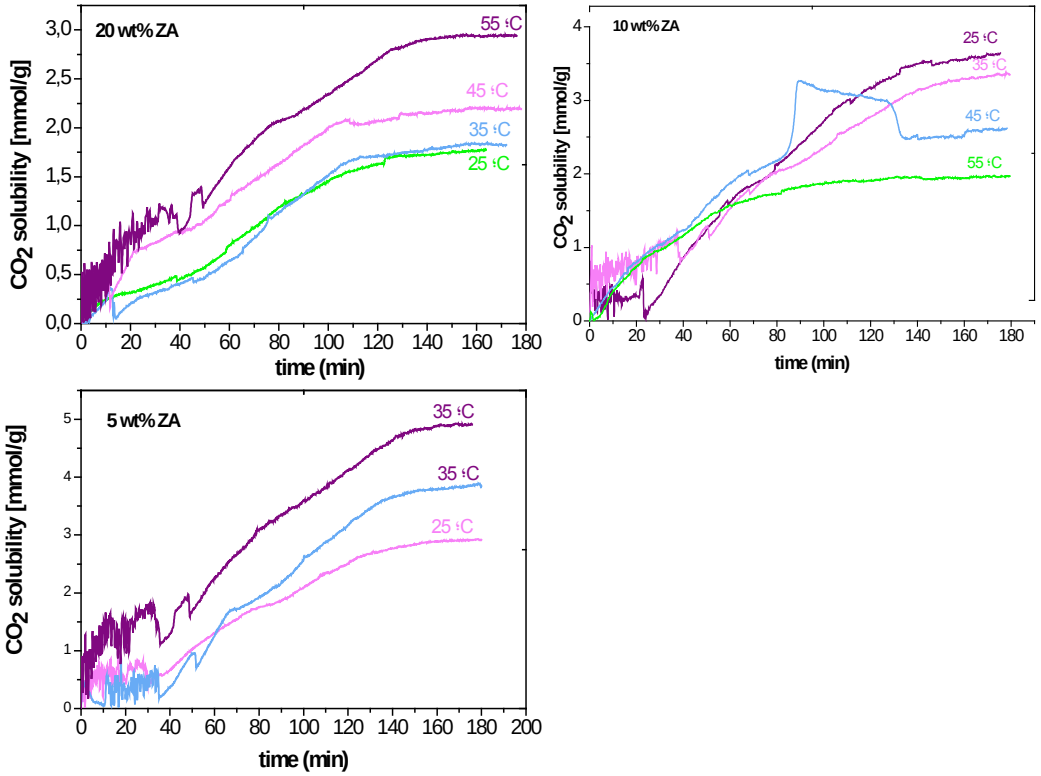

Figure 7. CO_2 adsorption curves of ZA-PTMSP membranes

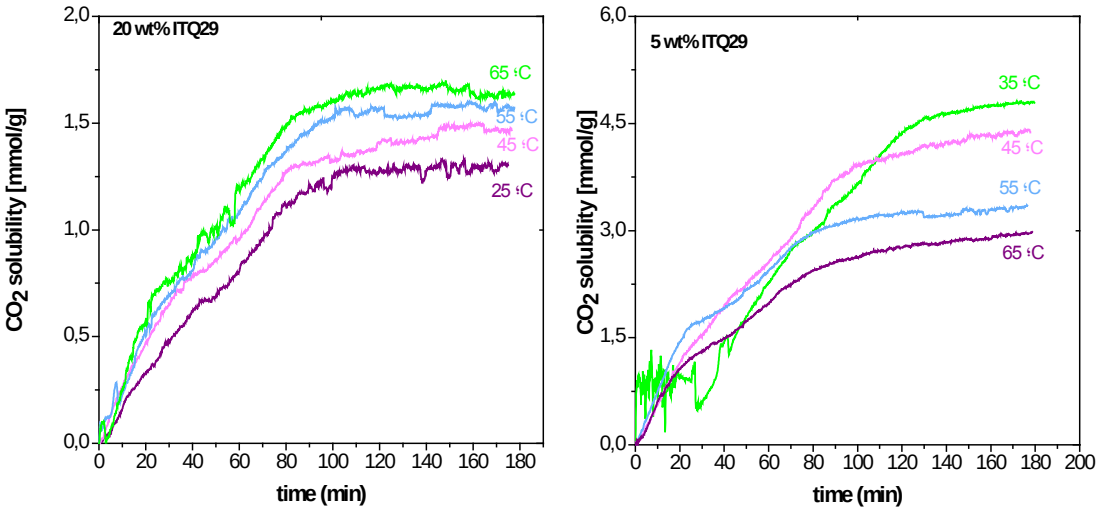

Figure 8. CO_2 adsorption curves of ITQ29-PTMSP membranes

The experimental results of adsorption behavior dependency for different loading of the zeolite A and zeolite ITQ29 in the MMMs are plotted in Figure 9 and Figure 10, respectively. By filling PTMSP with zeolite A, the CO_2 loading increased as compared with the pure PTMSP membrane. The CO_2 solubility improves with the loading of the zeolite A, being adsorbed almost 0.24 cm^3(STP)/cm^3-cmHg of CO_2 at 180 min of

experiment. However, when zeolite ITQ-29 is used as filler, the CO_2 solubility decreases with the loading of zeolite ITQ-29. This may be attributed to the lowest CO_2 sorption capacity of the hydrophobic pure silica ITQ-29, as compared with hydrophilic zeolite A [26].

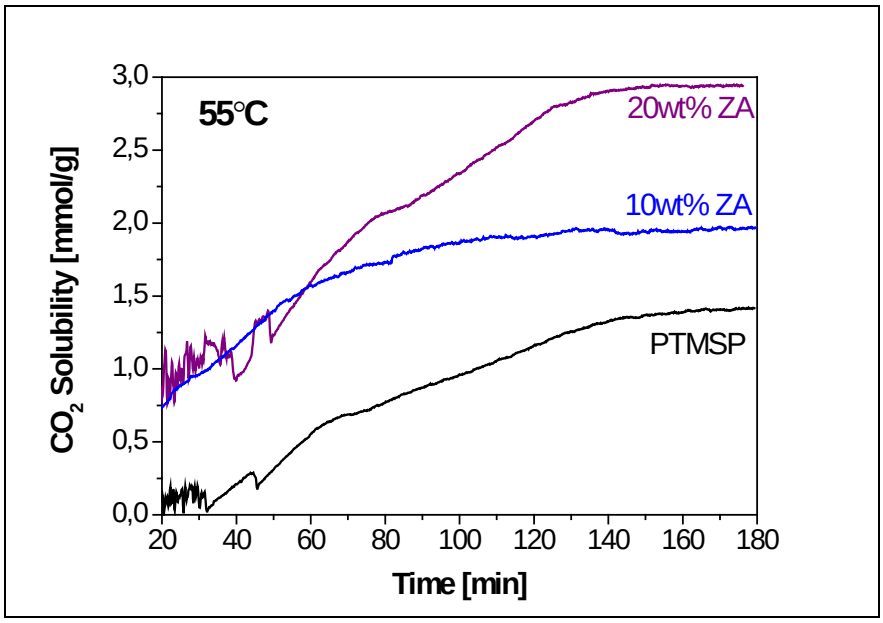

Figure 9. CO_2 adsorption curves of different PTMSP-ZA membranes at 55ºC

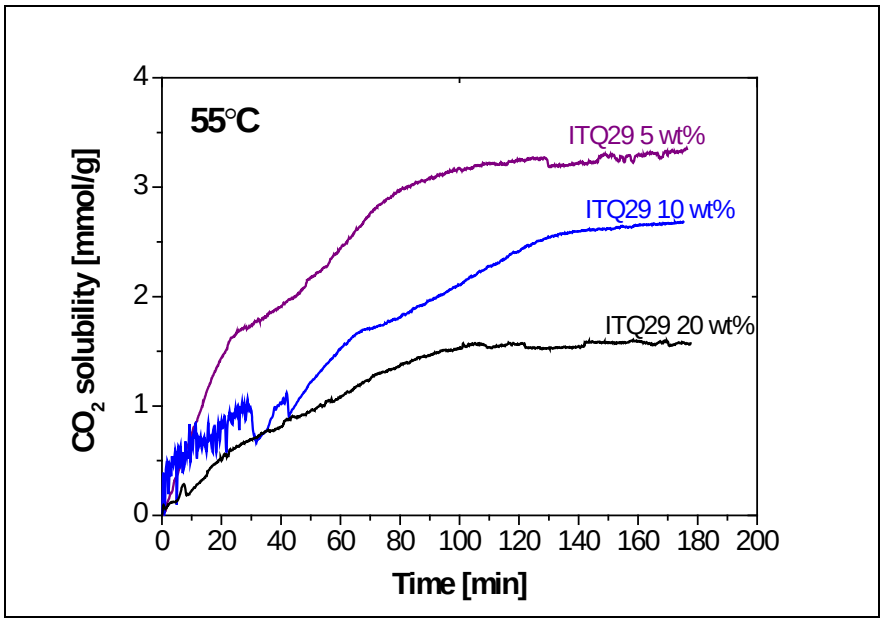

Figure 10. CO_2 adsorption curves of different PTMSP-ITQ29 membranes at 55ºC

The CO2 permeability values, as well as the CO_2/N_2 selectivities of the ZA-PTMSP and ITQ29-PTMSP membranes are shown in Table 3 and Table 4 respectively, as function

of temperature up to 60ºC. In the case of ZA-PTMSP membranes, the CO_2/N_2 selectivity increases with filler concentration due to the molecular sieving exerted by the incorporation of the zeolites in the membranes matrix. The selectivities obtained are considerably larger than for the pure polymer membrane, without compromising CO_2 permeabilities. When the zeolite dispersed is ITQ29, the greater selectivities are achieved when the filler concentration is low, that is, 5%. Besides, the increase of ITQ-29 zeolite loading decreases the CO_2 permeability.

Table 3. CO_2 permeability and CO_2/N_2 selectivity values for ZA -PTMSP- samples

Tª (ºC)	**PTMSP-ZA 5%**		**PTMSP-ZA 10%**		**PTMSP-ZA 20%**	
	P CO_2 (barrer)	**α CO_2/N_2**	**P CO_2 (barrer)**	**α CO_2/N_2**	**P CO_2 (barrer)**	**α CO_2/N_2**
25	12896 ± 5365	12.22 ± 1.11	284	0.25	10426 ± 6253	44.01 ± 35.21
30	12528 ± 3671	12.06 ± 1.74	4072	1.31	11803 ± 4560	45.22 ± 34.41
40	12306 ± 3823	12.66 ± 1.52	5625	2.51	14698 ± 2502	52.13 ± 21.32
50	11400 ± 3359	10.96 ± 1.35	13068	26.21	20961 ± 401	43.77 ± 7.32
60	11316	9.96	-	-	20071	19.60 ± 8.31

Table 4. CO_2 permeability and CO_2/N_2 selectivity values for ITQ-29-PTMSP- membranes

Tª (ºC)	**PTMSP-ITQ29 5%**		**PTMSP-ITQ29 10%**	
	P CO_2 (barrer)	**α CO_2/N_2**	**P CO_2 (barrer)**	**α CO_2/N_2**
25	3620 ± 2248	4.47 ± 0.52	1823	3.12
30	4215 ± 1896	4.85 ± 0.64	2056	3.43
40	5488 ± 1771	4.95 ± 0.99	2563	3.16
50	10842 ± 2690	7.56 ± 3.15	3475	4.40
60	15822 ± 2762	9.63 ± 2.53	4547	1.64

The permeation tests carried out at different temperature values allowed to evaluate the influence of this parameter on the transport properties of the membranes according to Eq. (3). The higher the temperature effect on the permeation rate is, the higher its energy activation value is.

The activation energies of permeation for CO_2 and N_2 are reported in Table 5. The activation energy for permeation of the MMMs increases with zeolite loading, because of the crosslinking [13].

The activation energies of CO_2 in pure PTMSP membranes are in good agreement with literature, which is usually dependent on the permeation set-up used for the measurements. PTMSP exhibits negative activation energies for all gases, due to the microporous structure [11].

Table 5. Apparent activation energy of permeation process for different gases (kJ/mol)

Membrane	CO_2	N_2
PTMSP	-7.10 ± 1.39	-12.63 ± 4.12
PTMSP-ZA 5 wt%	-3.25 ± 1.35	-4.41 ± 2.03
PTMSP-ZA 10 wt%	50.33	-73.96
PTMSP-ZA 20 wt%	17.21 ± 7.92	19.96 ± 10.7
PTMSP-ITQ29 5 wt%	35.90 ± 7.65	16.08 ± 1.53
PTMSP-ITQ29 10 wt%	22.51	38.15

In Figure 11 are the natural logarithms of CO_2 and N_2 permeability through pure PTMSP membranes plotted against the reciprocal of temperature. The solid lines are the linear regression of the data. In this case, permeability decreases with temperature indicating that activation energies of permeation are negative and following the typical behavior of PTMSP with temperature [11,12,24].

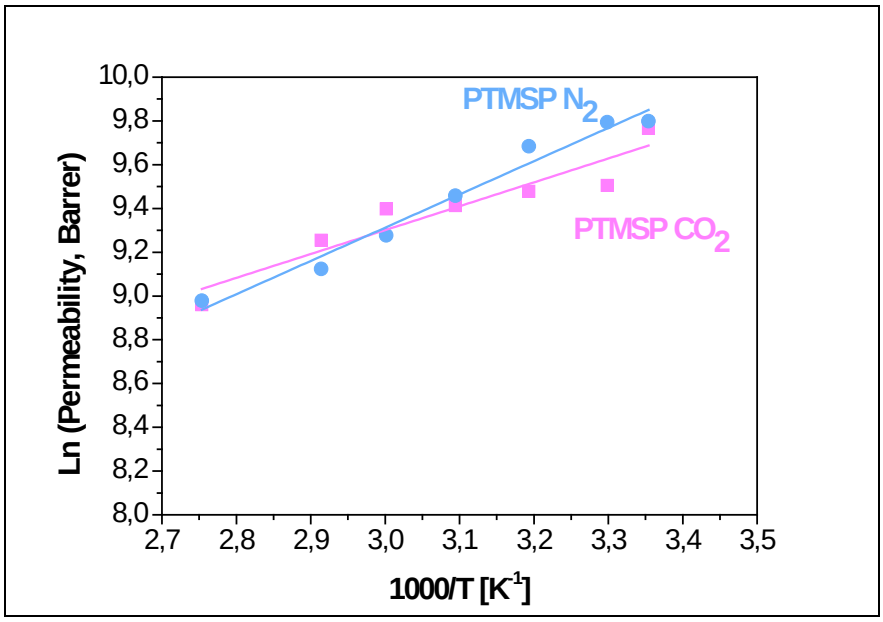

Figure 11. Permeability of carbon dioxide and nitrogen vs. reciprocal of temperature of pristine PTMSP membranes

For the 5 wt% ZA-PTMSP membranes, the permeability follows the same trend as the pure membranes, decreasing with temperature. However, when the loading of the filler is raised to 10 and 20 wt%, the CO_2 permeability changes its tendency and increases with temperature. This performance is also followed by the N_2 permeability in the 20 wt% ZA-PTMSP membranes (Figure 12). For the ITQ-29-PTMSP membranes, the CO_2 and N_2 permeabilities also increase with temperature (Figure 13).

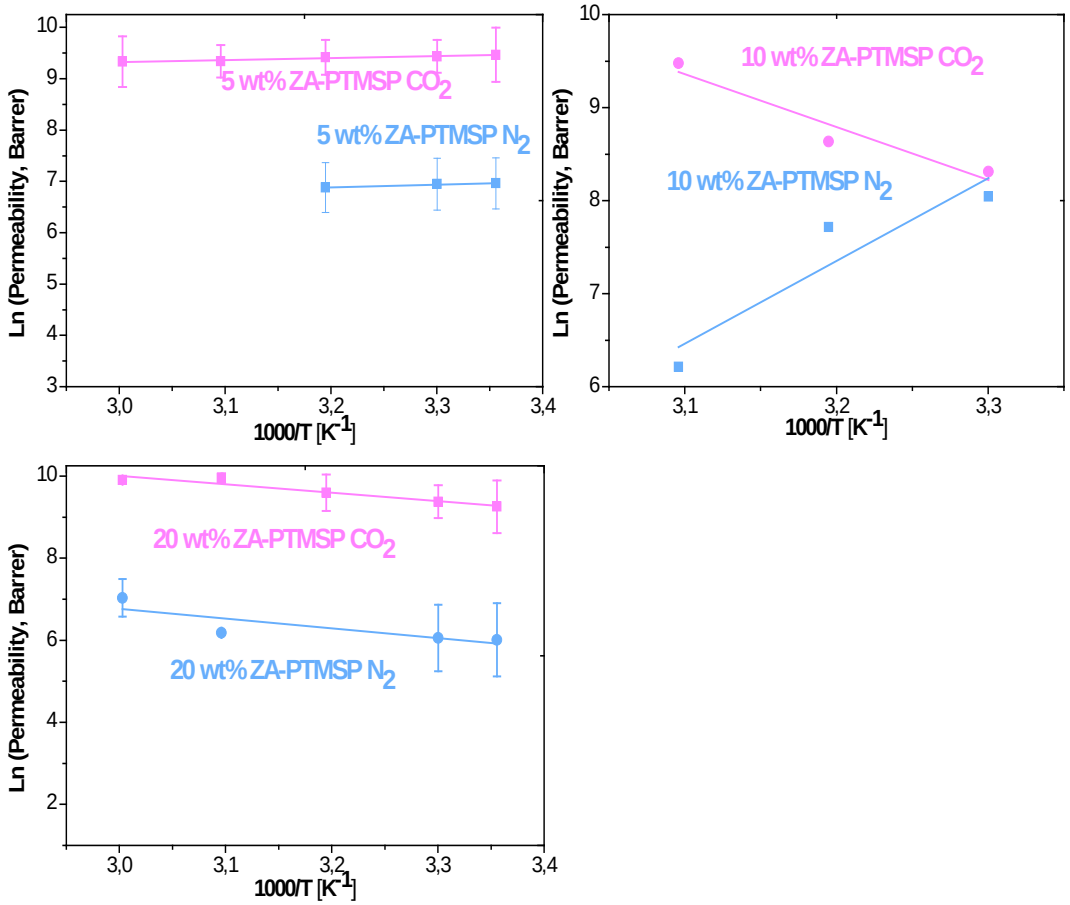

Figure 12. Permeability of CO_2 and N_2 vs. 1000/T of 5, 10 and 20 wt% ZA-PTMSP membranes

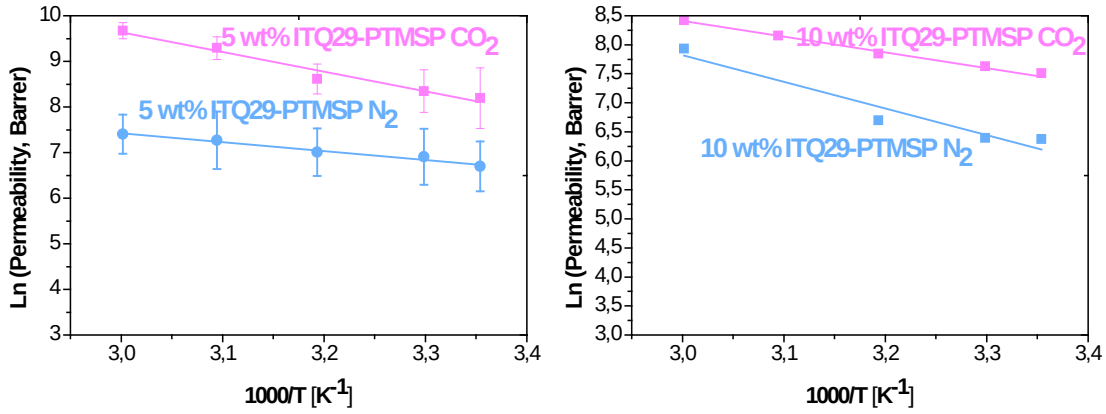

Figure 13. Permeability of CO_2 and N_2 vs. 1000/T of 5 and 10 wt% ITQ29-PTMSP membranes

In Figure 14, ZA-membranes are represented at the Robeson's upperbound plot. It can be observed that the more filler concentration, the better the permselectivity values. In fact, in the cases where zeolite loading is 10 and 20 wt%, the Robeson upperbound is overcome, being also very closed to it 5 wt% ZA-PTMSP membranes. Besides, the

permeabilities have not been reduced from pure PTMSP, in spite of the fact that in some works, permeabilities were lower for mixed matrix membranes than for pure polymer counterparts on account of the polymer chain rigidification with zeolite particles, the partial pore blockage of zeolites by the polymer chains and the extended diffusion pathways of the penetrants through the membrane [18]. In a high free volume glassy polymer such as PTMSP, the introduction of non-porous inorganic particles induces higher free volume for permeation [14]. In the case of zeolites, there is an additional porosity being introduced that can enhance this void fraction further. The non-ideal behavior observed at the highest loading of 20 wt.% may indicate that there are other voids appearing due to excessive loading of zeolites in the polymer matrix and this can induce defects that increase permeability and deteriorates selectivity.

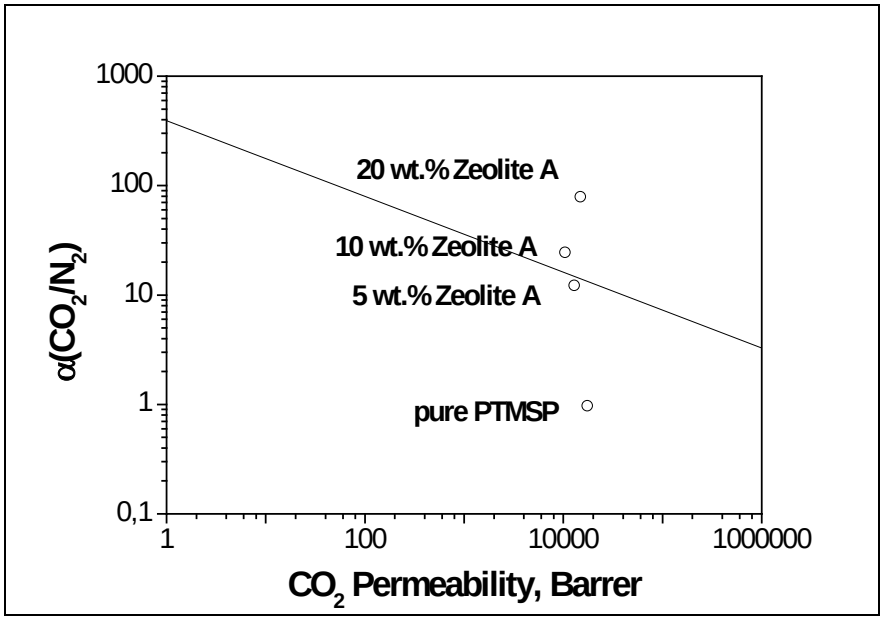

Figure 14. ZA-PTMSP membranes at Robeson plot at 25ºC

All glassy polymers, age physically, particularly those with high microporosity. Polymer aging is most prevalent in polymers with poor chain packing density that have exceptionally high fractional free volume (FFV) content. Previous studies show that PTMSP is a fast aging material, and increasing temperature will accelerate physical aging, which will increase density. Over time, the packing density increases, and the permeability drops dramatically [12,25]. It should be noted that physical aging in PTMSP could be reversed by soaking the polymer in a swelling solvent like methanol. In this work, membranes have been immersed in methanol prior to each experiment, in order to control physical aging. In Table 6 the compaction values of different

membranes are calculated as the difference on the membrane density before and after the set of permeation experiments. It can be observed that the density of the membranes increase with the introduction of the zeolites, which results in a physical aging reduction, revealed by a reduction of the degree of compaction when zeolite loading is increased from 0 to 10 wt%. The compaction increased to 31 % at 20 wt% zeolite loading, thus implying that this concentration is excessive, related to voids and defects and the non-ideal performance observed on Figure 15 and Figure 16.

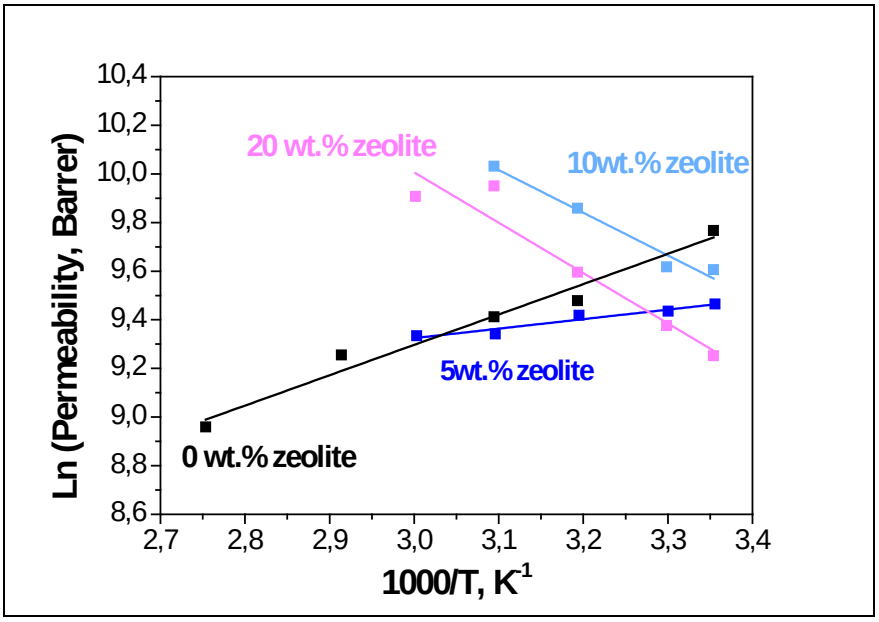

Figure 15. Temperature dependence on CO_2 permeability

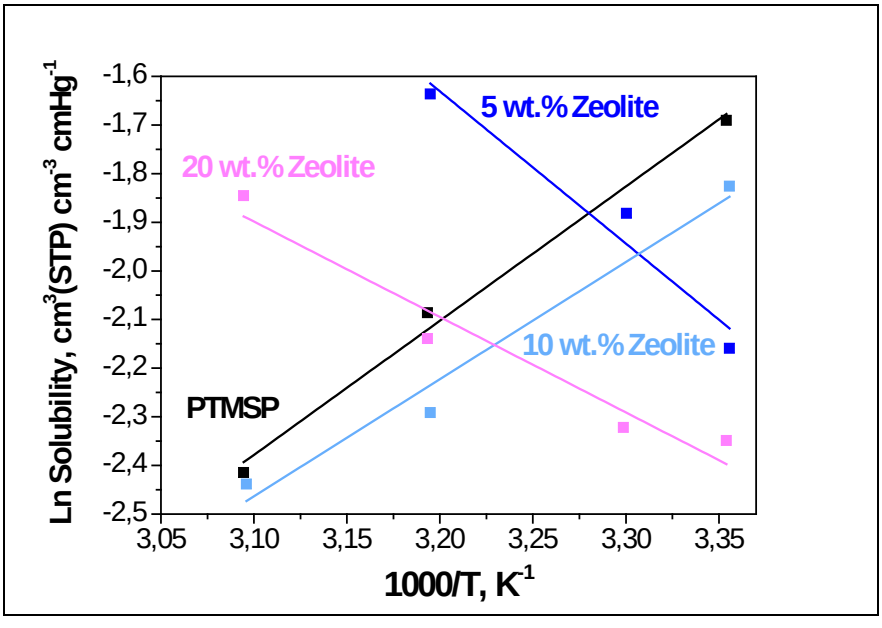

Figure 16. Temperature dependence on CO_2 solubility

Table 6. Compaction values of different membranes

	Density (g/cm_3) Before permeation	Density (g/cm_3) After permeation	Compaction (%)
Pure PTMSP	0.692 ±0.08	0,587±0,07	10,53 ± 5,2
5 wt% ZA-PTMSP	0,692 ± 0,12	0,628±0,08	6,32 ± 4,2
10 wt% ZA-PTMSP	0,608±0,00	0,574±0,00	3,4 ± 0,10
20 wt% ZA-PTMSP	0,900	0,585	31,5

In Figure17, the experimental results of ZA-PTMSP membranes at 30 ºC are compared with the predicted by the Maxwell model. It can be seen that experimental results are higher than those predicted by Maxwell model, thus implying that this model is not sufficient to describe the physical phenomena occurring in this material. On the one hand, the Maxwell model is generally only valid for low dispersed filler concentrations in the continuous phase or polymer membrane, and on the other, the results showed in this work revealed so far non-idealities in the MMMs that have to be further studied. Besides, the influence of temperature on MMMs performance seems to be decisive in the membranes developed here and this has not been predicted yet by MMM models that are based on Maxwell equation.

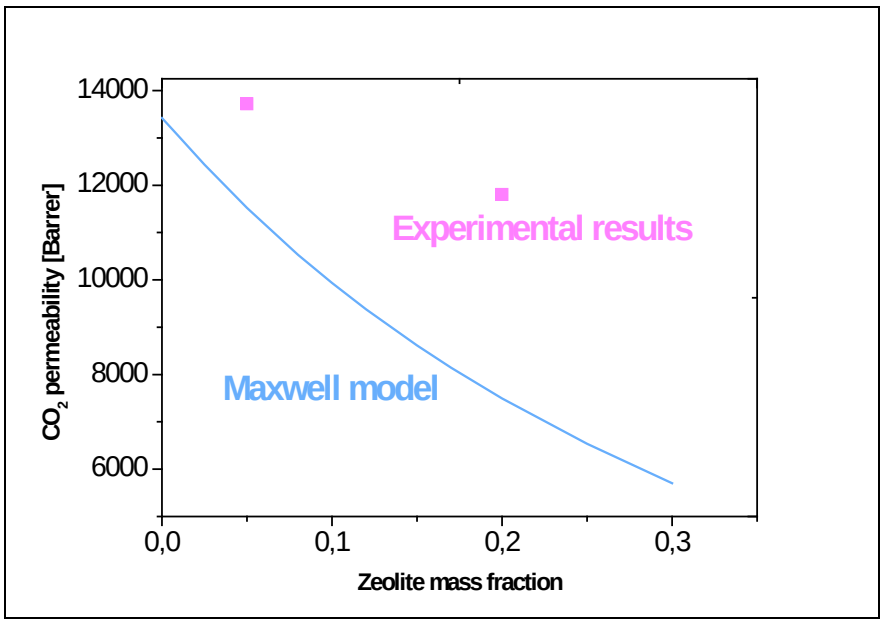

Figure17. Comparison of Maxwell model with experimental results

4. Conclusions

Mixed Matrix Membranes (MMMs) were prepared using highly permeable PTMSP polymer and small pore LTA-type zeolites with different Si/Al ratio and different compositions by the solution-casting method. The resulting MMMs presented high thermal stability and good interaction.

The permeability and selectivity of the MMMs is higher than pure polymer membranes due to the molecular sieving effect imparted by the introduction of the small-pore zeolite and the good interaction between polymer and zeolite in the membrane matrix, overcoming existing polymer materials performance (Robeson's). Better results were obtained using zeolite A than using ITQ-29.

The incorporation of the zeolites in the membrane matrix reduces physical aging.

The use of increasing temperature in zeolite/PTMSP MMMs enhanced CO_2/N_2 permselectivity performance by introducing additional transport mechanisms that have yet to be described, because the Maxwell equation does not adequately predict the gas separation performance of the novel MMM developed in this work.

5. Acknowledgements

Financial support from the Spanish Ministry of Economy and Competitiveness (MINECO) under project CTQ2012-31229 at the Universidad de Cantabria is gratefully acknowledged.

6. References

[1] S.C. Page, A.G. Williamson, and I.G. Mason. Carbon capture and storage: Fundamental thermodynamics and current technology. Energy Policy, 37 (2009) 3314.

[2] R. Stuart Haszeldine. Carbon capture and storage: how green can black be? Science, 325 (2009) 1647.

[3] E. Favre. Carbon dioxide recovery from post-combustion processes: Can gas permeation membranes compete with absorption? J.Membr.Sci., 294 (2007) 50.

[4] H. Lin, B.D. Freeman. Materials selection guidelines for membranes that remove CO_2 from gas mixtures. J.Mol.Struct., 739 (2005) 57.

[5] J. Gascon, F. Kapteijn, B. Zornoza, V. Sebastián, C. Casado, and J. Coronas. Practical approach to zeolitic membranes and coatings: State of the art, opportunities, barriers, and future perspectives. Chemistry of Materials, 24 (2012) 2829.

[6] K. Ramasubramanian, Y. Zhao, and W.S. Winston Ho. CO_2 capture and H2 purification: Prospects for CO_2-selective membrane processes. AIChE J., 59 (2013) 1033.

[7] L.M. Robeson. The upper bound revisited. J.Membr.Sci., 320 (2008) 390.

[8] T.-. Chung, L.Y. Jiang, Y. Li, and S. Kulprathipanja. Mixed matrix membranes (MMMs) comprising organic polymers with dispersed inorganic fillers for gas separation. Progress in Polymer Science (Oxford), 32 (2007) 483.

[9] K. Nagai, T. Masuda, T. Nakagawa, B.D. Freeman, and I. Pinnau. Poly[1-(trimethylsilyl)-1-propyne] and related polymers: Synthesis, properties and functions. Progress in Polymer Science (Oxford), 26 (2001) 721.

[10] S. Matteucci, V.A. Kusuma, D. Sanders, S. Swinnea, and B.D. Freeman. Gas transport in TiO2 nanoparticle-filled poly(1-trimethylsilyl-1-propyne). J.Membr.Sci., 307 (2008) 196.

[11] T.C. Merkel, R.P. Gupta, B.S. Turk, and B.D. Freeman. Mixed-gas permeation of syngas components in poly(dimethylsiloxane) and poly(1-trimethylsilyl-1-propyne) at elevated temperatures. J.Membr.Sci., 191 (2001) 85.

[12] A. Morisato, H.C. Shen, S.S. Sankar, B.D. Freeman, I. Pinnau, and C.G. Casillas. Polymer characterization and gas permeability of poly(1-trimethylsilyl-1-propyne) [PTMSP], poly(1-phenyl-1-propyne) [PPP], and PTMSP/PPP blends. J.Polym.Sci.Part B, 34 (1996) 2209.

[13] J.-. Qiu, C.-. Liu, F. Hu, X.-. Guo, and Q.-. Zheng. Synthesis of unsaturated polyphosphoester as a potential injectable tissue engineering scaffold materials. J Appl Polym Sci, 102 (2006) 3095.

[14] M. Woo, J. Choi, and M. Tsapatsis. Poly(1-trimethylsilyl-1-propyne)/MFI composite membranes for butane separations. Microporous and Mesoporous Materials, 110 (2008) 330.

[15] B. Zornoza, P. Gorgojo, C. Casado, C. Téllez, and J. Coronas. Mixed matrix membranes for gas separation with special nanoporous fillers. Desalination and Water Treatment, 27 (2011) 42.

[16] R. Mahajan, W.J. Koros. Factors controlling successful formation of mixed-matrix gas separation materials. Industrial and Engineering Chemistry Research, 39 (2000) 2692.

[17] C. Casado-Coterillo, J. Soto, T.M. Jimaré, S. Valencia, A. Corma, C. Téllez, et al. Preparation and characterization of ITQ-29/polysulfone mixed-matrix membranes for gas separation: Effect of zeolite composition and crystal size. Chemical Engineering Science, 73 (2012) 116.

[18] D. Sen, H. Kalipçilar, and L. Yilmaz. Development of polycarbonate based zeolite 4A filled mixed matrix gas separation membranes. J.Membr.Sci., 303 (2007) 194.

[19] M.M. Lozinska, J.P.S. Mowat, P.A. Wright, S.P. Thompson, J.L. Jorda, M. Palomino, et al. Cation gating and relocation during the highly selective "trapdoor"

adsorption of CO_2 on univalent cation forms of zeolite Rho. Chemistry of Materials, 26 (2014) 2052.

[20] A. Urtiaga, E.D. Gorri, C. Casado, and I. Ortiz. Pervaporative dehydration of industrial solvents using a zeolite NaA commercial membrane. Separation and Purification Technology, 32 (2003) 207.

[21] J.E. Bara, S. Lessmann, C.J. Gabriel, E.S. Hatakeyama, R.D. Noble, and D.L. Gin. Synthesis and performance of polymerizable room-temperature ionic liquids as gas separation membranes. Industrial and Engineering Chemistry Research, 46 (2007) 5397.

[22] E.L. Cussler , Diffusion. Mass transfer in fluid systems, in Anonymous , 3rd ed. Cambridge University Press, 2007, pp. 631.

[23] M. Hussain, A. König. Mixed-Matrix Membrane for Gas Separation: Polydimethylsiloxane Filled with Zeolite. Chemical Engineering and Technology, 35 (2012) 561.

[24] X.-. Wang, A.J. Hill, B.D. Freeman, and I.C. Sanchez. Structural, sorption and transport characteristics of an ultrapermeable polymer. J.Membr.Sci., 314 (2008) 15.

[25] C.H. Lau, P.T. Nguyen, M.R. Hill, A.W. Thornton, K. Konstas, C.M. Doherty, et al. Ending aging in super glassy polymer membranes. Angewandte Chemie - International Edition, 53 (2014) 5322.

[26] M. Palomino, A. Corma, F. Rey, and S. Valencia. New insights on C02-methane separation using LTA zeolites with different Si/Al ratios and a first comparison with MOFs. Langmuir, 26 (2010) 1910.

Departamento de Ingenierías Química
y Biomolecular
Universidad de Cantabria (SPAIN)

DEVELOPMENT OF HIGHLY PERMEABLE, SELECTIVE AND ROBUST MEMBRANE MATERIALS FOR CO_2 SEPARATION

Author: Ana Fernández Barquín

Advisor: Clara Casado Coterillo

Máster en Ingeniería química: "Producción y Consumo Sostenible"

11th July 2014

Outline

1. Background

Climate change: Carbon capture and storage

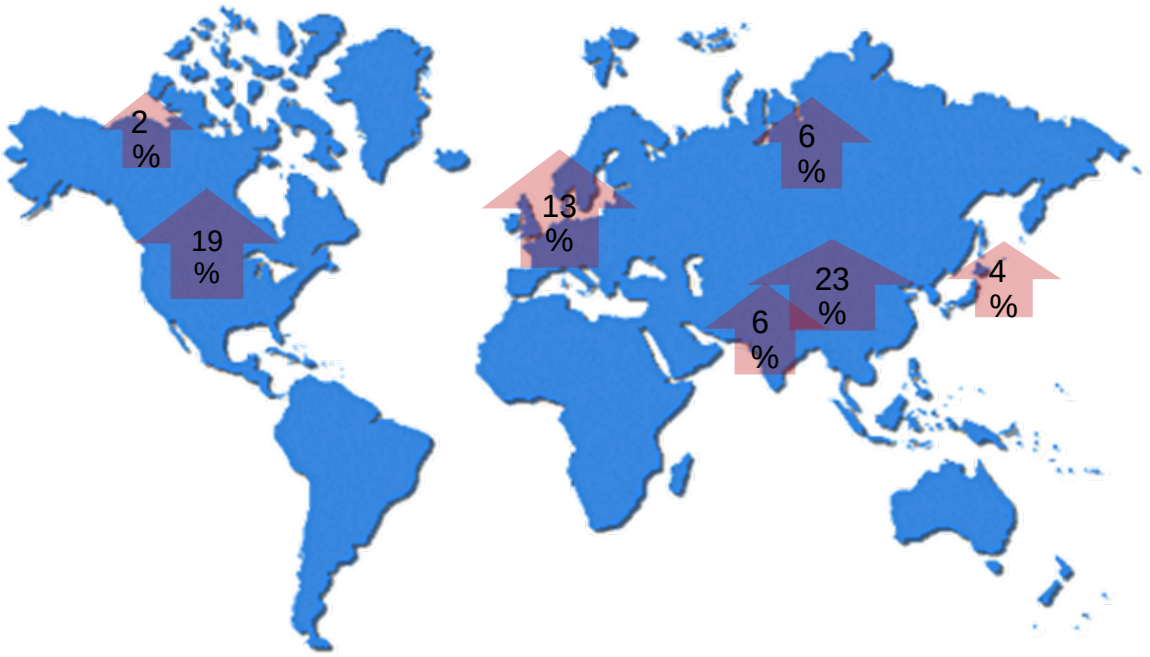

Table 1. Strategies to reduce CO_2 content [2]

Strategy	Target mixture	Conditions	Conventional separation process	Membrane opportunity
Oxycombustion	O_2/N_2	Atmospheric P Room temperature	Cryogenics	ITM
Precombustion	H_2/CO_2	P ≤ 80 bar T = 300-500ºC	G-L Physical absorption	Membrane reactor
Postcombustion	CO_2/N_2	Atmospheric P T = 100 – 200ºC	G-L chemical absorption	Membrane separations

[1] 2008 Global CO_2 Emissions from Fossil Fuel Combustion and some Industrial Processes (million metric tons of CO_2)
[2] Czyperek et al 2010. J. Membr. Sci. 2010. 359: 149-159.

1. Background

Membrane technology

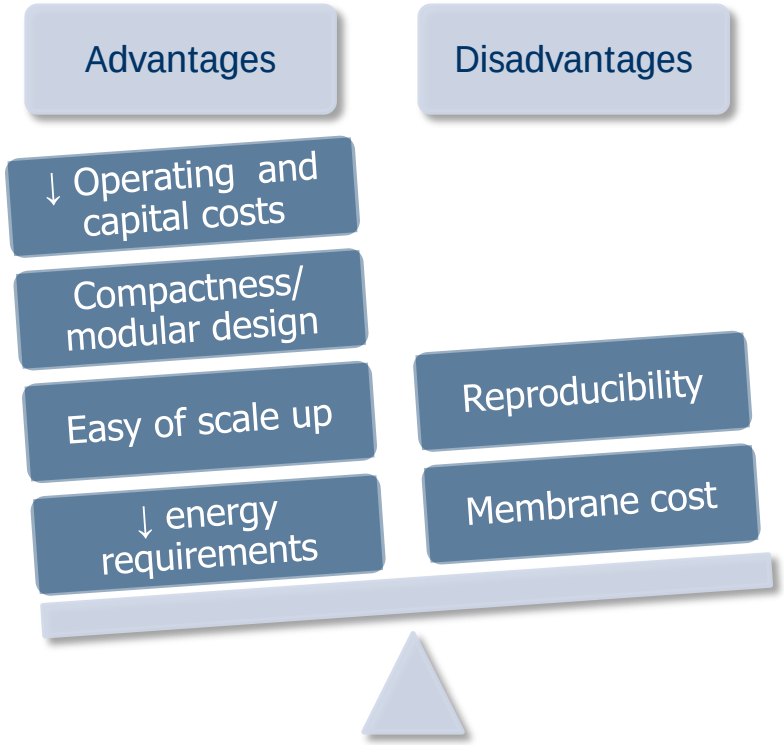

Industrial gas separation applications

- ❖ Good performance
- ❖ Robust enough for long term operations
- ❖ High permeability
- ❖ Good selectivity

Table 2. Commercial polymeric membranes for CO_2 capture

Membrane (Supplier)	Membrane material
Polyactive ® (GKSS)	Silicone rubber
PDMS 4060 (Sulzer)	Polydimethylsiloxane
Separex (UOP)	Cellulose acetate
Polaris ® (MTR)	Silicone rubber

- ✓ *Commercially available*
- ✓ *Low cost*
- ✓ *Reproducibility*

- ✗ *Thermal , mechanical and chemical resistance*
- ✗ *Durability in effluents containing water vapour*
- ✗ *CO_2 plasticization*

1. Background

Poly[1-(trimethylsilyl)-1-propyne)] (PTMSP)

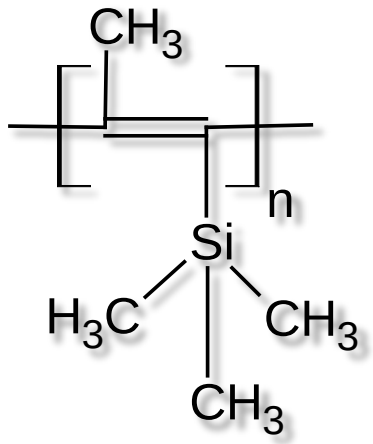

- Glassy polymer
- Tg > 250 ºC
- Low chain mobility
- Low density (0.75 g/cm^3)
- Large free volume (0.29)
- Most permeable polymer

Permeability

Trade off

Selectivity

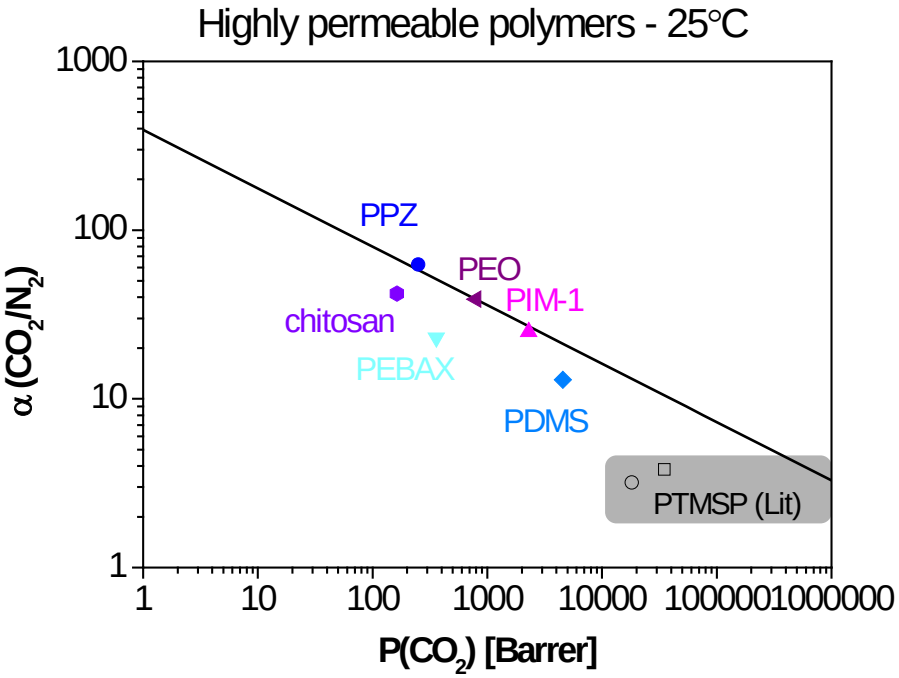

1. Background

Mixed Matrix Membranes

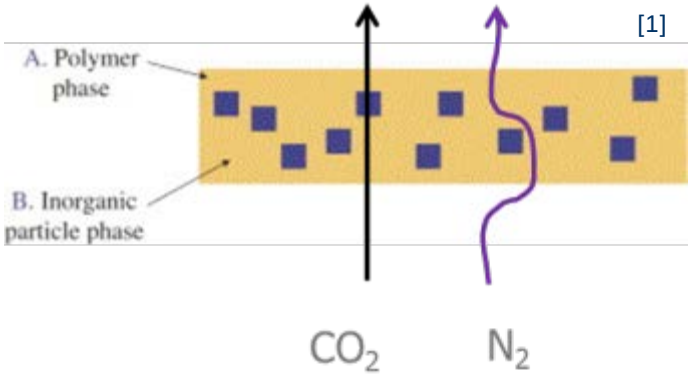

Combine

- Molecular sieving effect and catalytic properties of inorganic fillers
- Mechanical properties and economical processing capacity of polymers

Typical inorganic fillers:

- Zeolites
- Activated carbons
- Carbon molecular sieves
- Non-porous silica
- Graphite

Blending a polymer with inorganic filler may enhance the properties of both materials on membrane gas separation.

Major challenge: adhesion/interaction between components

[1] T.-S. Chung, L.Yet al., 2007. Prog. Pol. Sci., 32. 483-507.

1. Background

Zeolite molecular sieves

Zeolites are crystalline aluminosilicates, hydrated, microporous structures composed of AlO_4 and SiO_2 tetrahedra.

- Regular structure
- Molecular size close to molecules
- High thermal and chemical stability
- High specific surface and adsorption properties
- Catalytic activity
- Ion exchange capacity

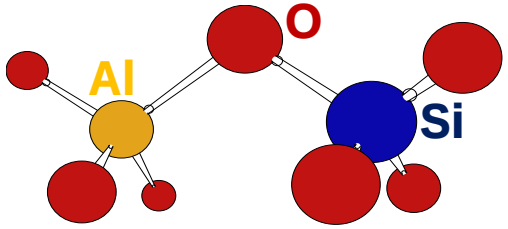

$M_{x/n}[(AlO_2)_x(SiO_2)_y]\cdot z\ H_2O$

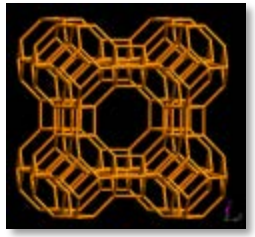

Zeolite LTA type

Chabazite 2

Mordenite 10-40

ZSM-5 20-1000

Zeolite A 1

Si/Al ratio

hydrophilicity

ITQ-29 silicalite ∞

2. Objectives

- ✓ Preparation of MMM using PTMSP and small pore LTA-type zeolites with different Si / Al ratio and varying the loading of zeolite

- ✓ Structural characterization of membrane materials using XRD as well as heat resistance and solubility of the membrane to CO_2.
  Measurement of CO_2 and N_2 permeation at temperatures in the range 25 – 100 ºC

- ✓ Analysis of results, comparing the permeability and selectivity data in Robeson plot and studying the influence of temperature and composition.

3. Experimental methodology

Polymer and mixed matrix membrane preparation

Polymer:	Poly(1-trimethylsilyl-1-propyne)
Inorganic filler:	❖ Commercial zeolite A (Si/Al = 1) ❖ ITQ-29 (Si/Al = ∞) ❖ Particle size = 4.5 µm
Solvent:	Toluene
Reaction conditions:	Refluxing 60ºC 24h
Method	Solution casting
Drying	❖ Slow at room temperature ❖ Removal from glass plate ❖ Inmersion in methanol

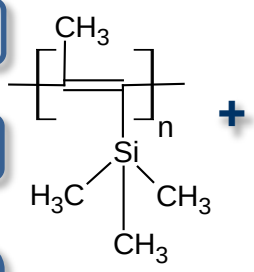

+

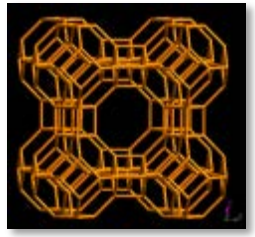

3. Experimental methodology

Membrane characterisation: Gas permeation

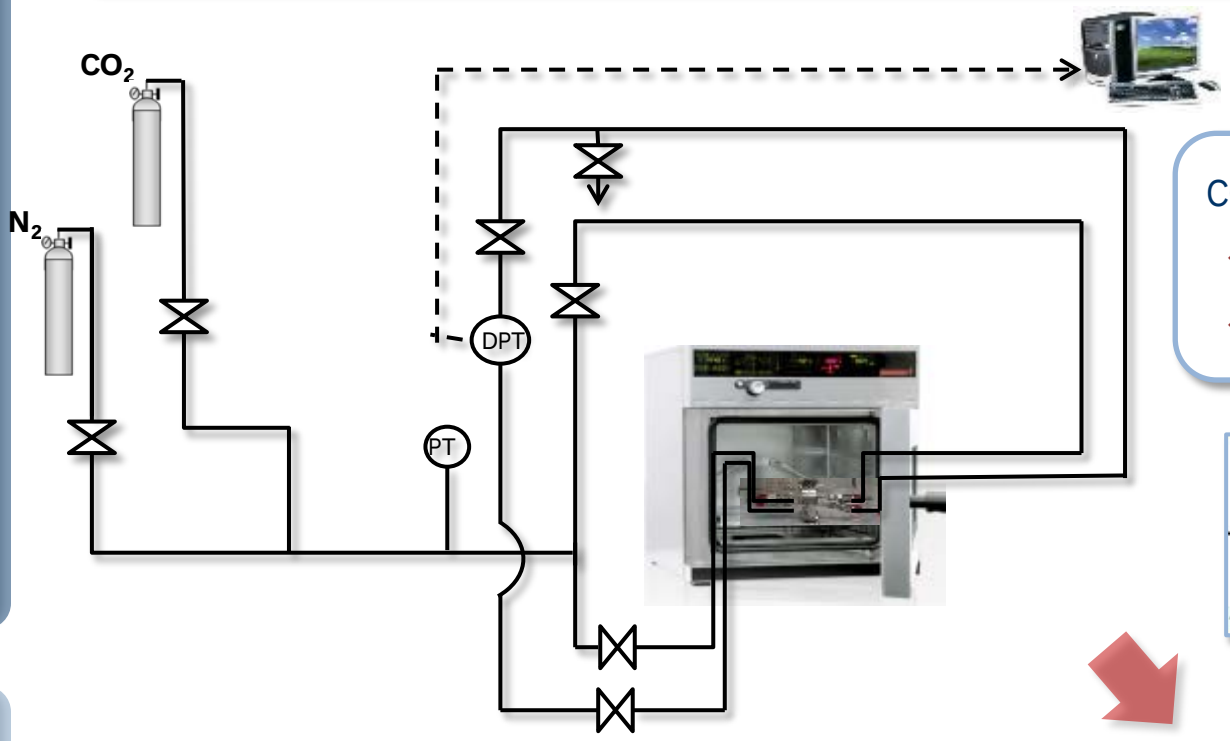

CO_2 and N_2 permeation test

- 25 – 100ºC
- 2 – 3 bar

$$\frac{1}{\beta_m} ln\left(\frac{\Delta p_0}{\Delta p}\right) = P\frac{t}{l}$$

P(T)

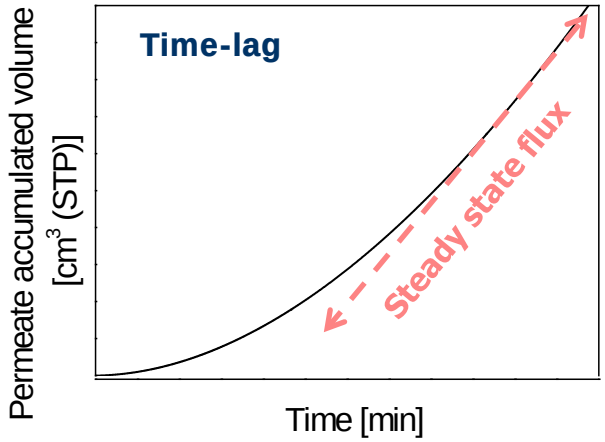

$$D = \frac{l^2}{6\theta}$$

D(T)

3. Experimental methodology

Membrane characterisation: Thermogravimetrical analysis

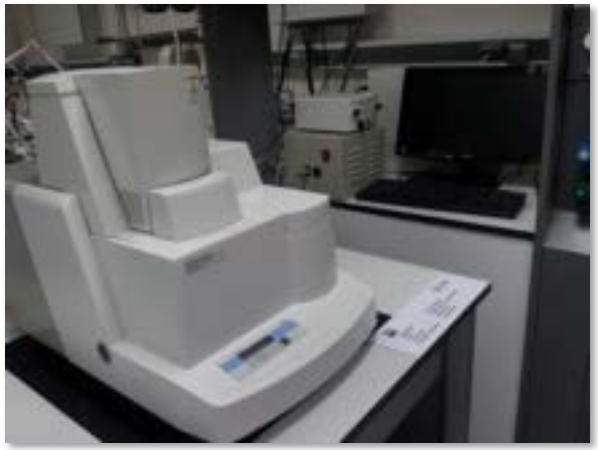

(DTG-60H, SHIMADZU, Japan)

- CO_2 adsorption for 180 min at 25 – 60ºC
- TGA in air at 10ºC/min up to 700 ºC

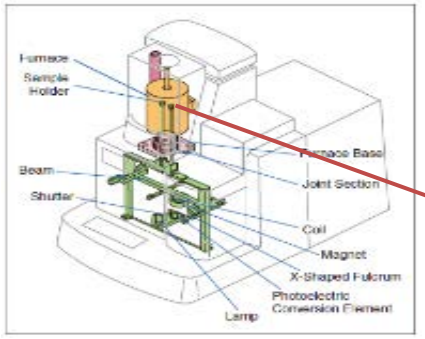

High sensivity

DTA detectors

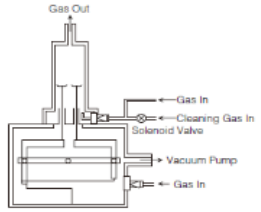

Membrane characterisation: X-ray diffraction analysis

(Philips X'Pert PRO MPD diffractometer)

- 45 kV and 40 mA
- Cu Kα1 radiation (λ = 1.5406 Å)
- Solid angle detector, at a step of 0.05º

3. Results

X-ray diffraction analysis

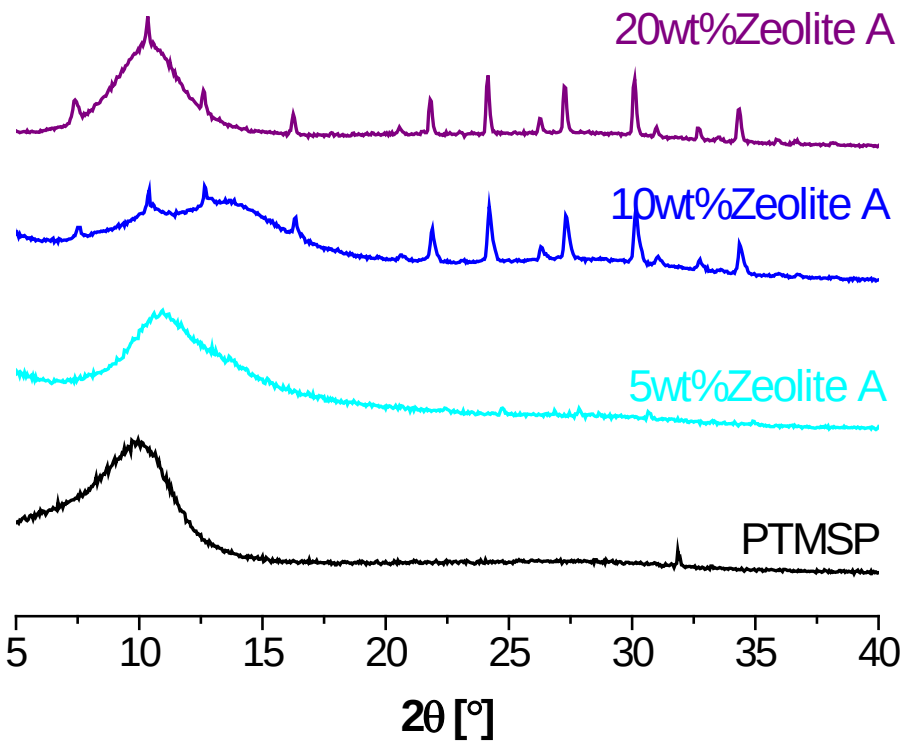

The X-ray diffraction (XRD) patterns of the films discern a good interaction between the zeolite and the polymer matrix .The characteristic reflections of zeolite A become stronger upon loading increase

3. Results

Thermal stability

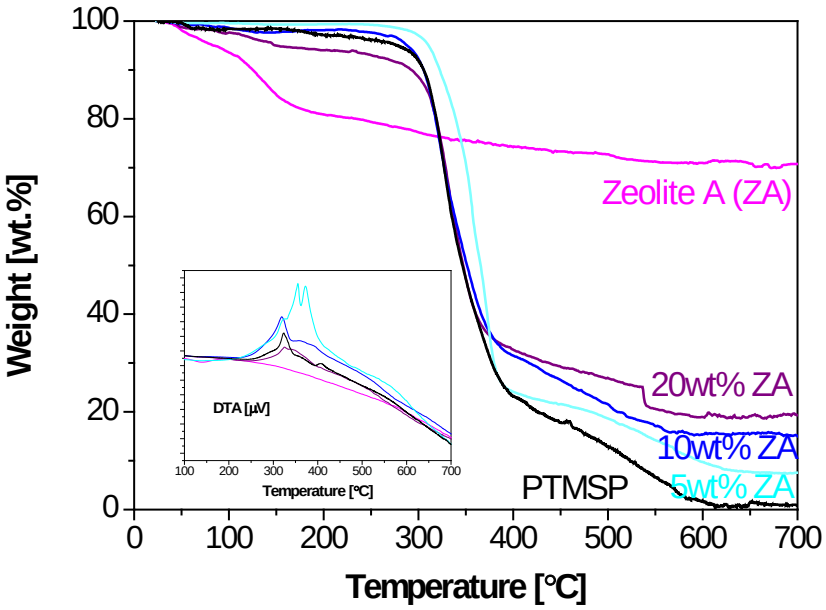

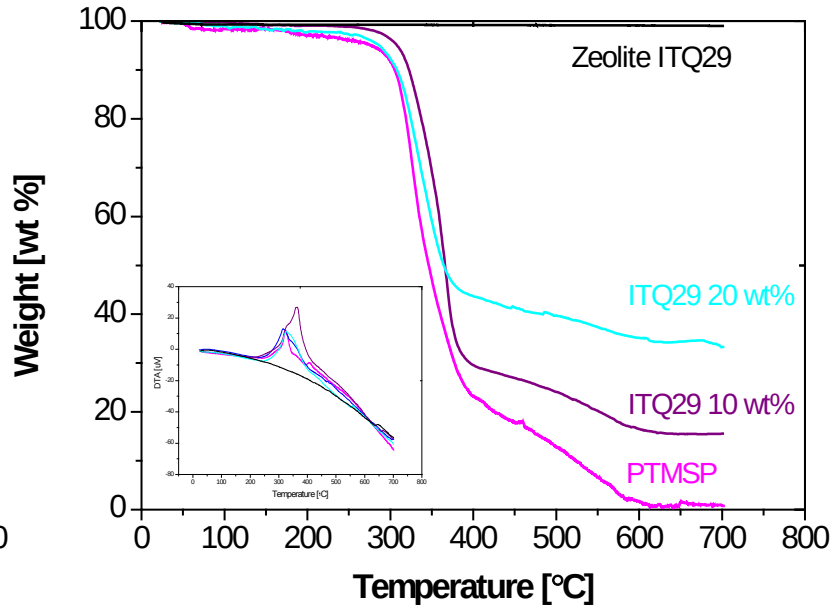

The real zeolite loading of PTMSP membranes obtained by TGA agreed with nominal value; the thermal stability of the membranes is similar to the glassy polymer PTMSP.

3. Results

CO_2 adsorption

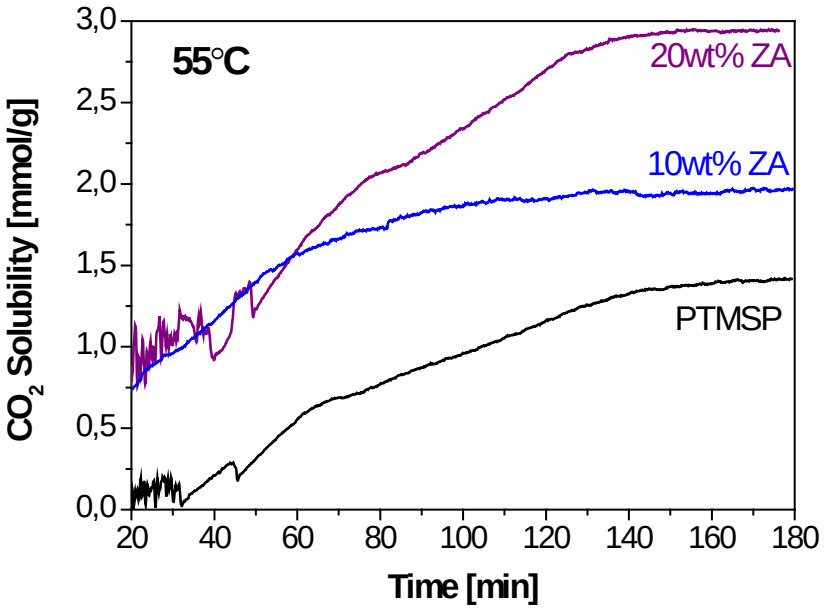

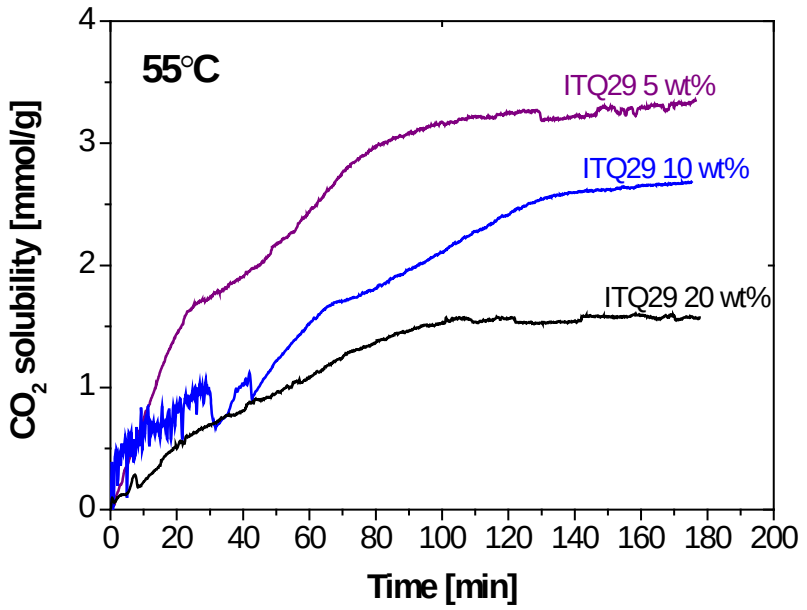

By filling PTMSP with zeolite A, the CO_2 loading increased as compared with the pure PTMSP membrane. With zeolite ITQ-29 as filler, CO_2 solubility decreases with loading of zeolite ITQ-29

3. Results

Gas permeation through Zeolite/PTMSP MMM

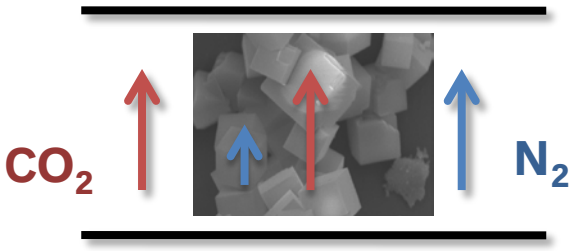

- Temperature = 25ºC
- $P_{upstream}$ = 310 kPa
- $P_{downstream}$ = 100 kPa

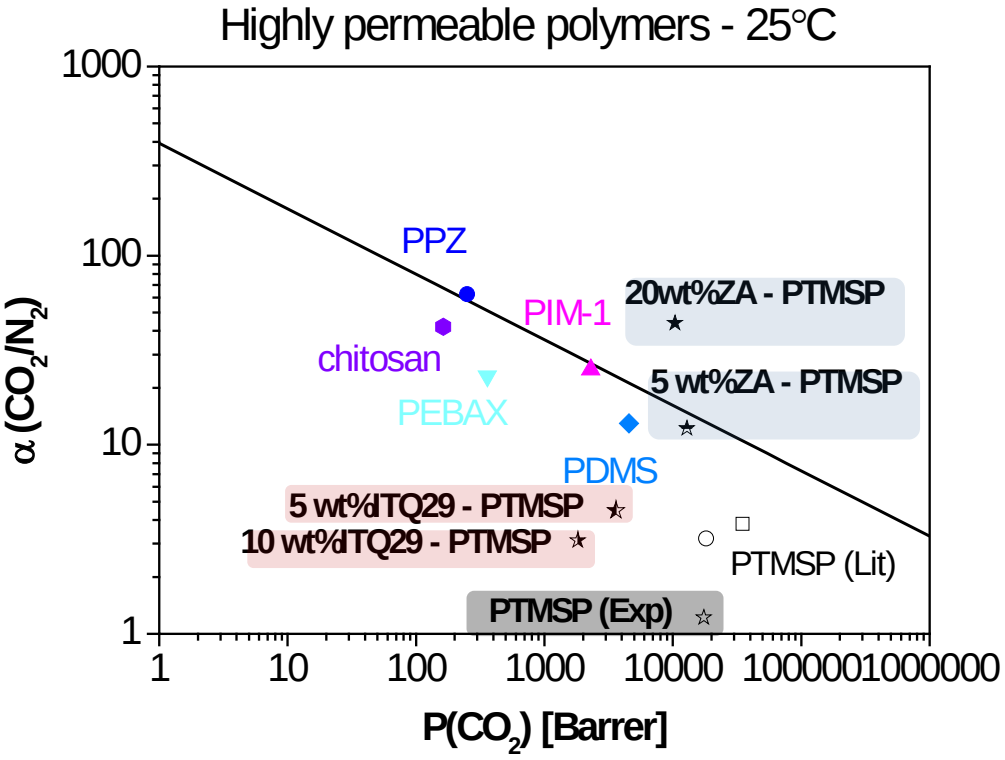

The selectivity of PTMSP increases with the incorporation of small pore zeolite loading without remarkable decrease in permeability, overcoming existing polymer materials performance.

3. Results

Influence of T^a in permeation of CO_2 and N_2 through MMMs

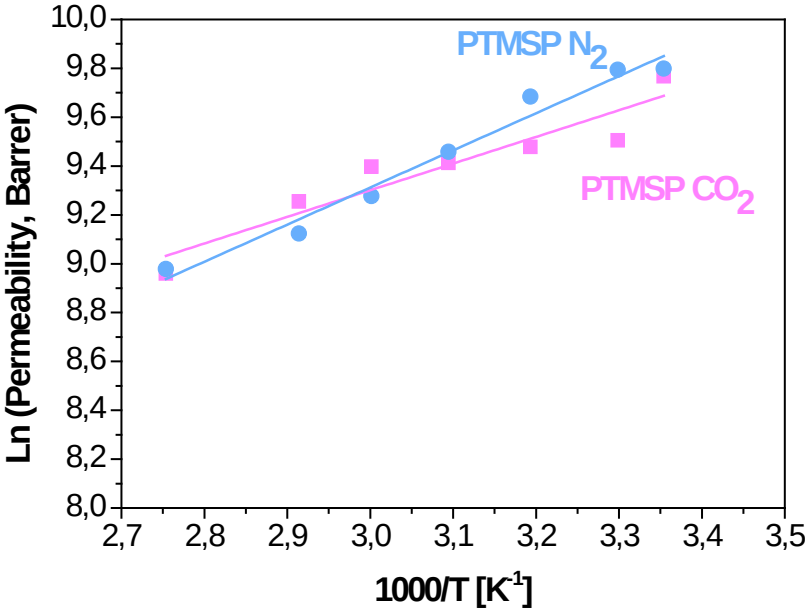

Table 3. Apparent activation energy of permeation process (kJ/mol)

Membrane	CO_2	N_2
PTMSP	-7.10	-12.63
PTMSP-ZA 5 wt%	-3.25	-4.41
PTMSP-ZA 20 wt%	17.21	19.96
PTMSP-ITQ29 5 wt%	35.90	16.08
PTMSP-ITQ29 10 wt%	22.51	38.15

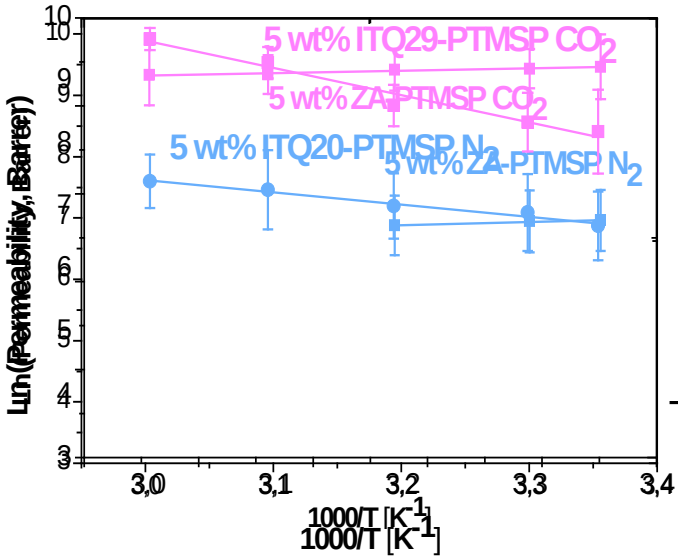

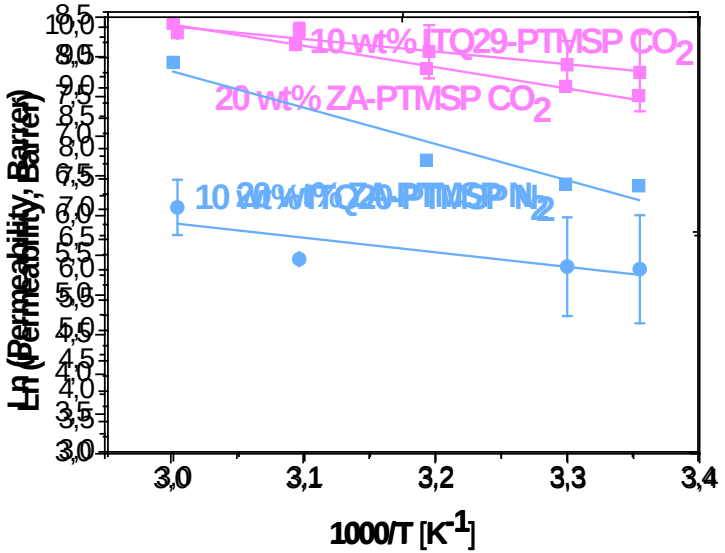

3. Results

Study of physical aging

- Increasing T^a
- Accelerate physical aging
- Increase density
- The permeability drops

Table 4. Compaction values of different membranes

	Compaction (g/cm3)
Pure PTMSP	0,042 ± 0,031
5 wt% ZA-PTMSP	0,063 ± 0,042
10 wt% ZA-PTMSP	0,034 ± 0,001
20 wt% ZA-PTMSP	0,315

Physical aging in PTMSP could be reversed by soaking the polymer in a swelling solvent like methanol

The density of the membranes increases with the introduction of the zeolites, which results in a physical aging reduction.

3. Results

Maxwell model

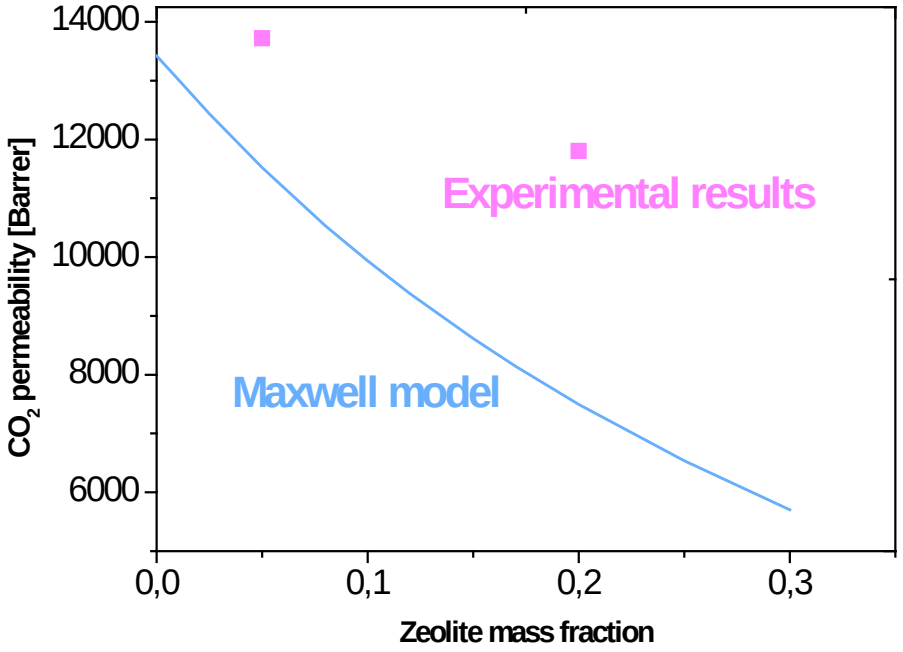

Experimental results higher than those predicted by Maxwell model

$$P_{eff} = P_c \cdot \frac{P_d + 2P_c - 2\emptyset(P_c - P_d)}{P_d + 2P_c + \emptyset(P_c - P_d)}$$

Where:

Peff :effective composite membrane permeability

Φ : Volume fraction

P: single component permeability

d: disperse phase

c: continuous phase

Conclusions

MMMs were prepared using highly permeable PTMSP polymer and small pore LTA-type zeolites with different Si/Al ratio and different compositions by the solution-casting method. The resulting MMMx presented high thermal stability and good interaction.

The permeability and selectivity of the MMMs is higher than pure polymer membranes due to the molecular sieving effect imparted by the introduction of the small-pore zeolite and the good interaction between polymer and zeolite in the membrane matrix, overcoming existing polymer materials performance (Robeson's).

The use of increasing temperature enhanced CO_2/N_2 permselectivity performance and the incorporation of tzhe zeolites in the membrane matrix reduces physical aging.

Experimental results are higher than those predicted by Maxwell model, thus implying that this model is not sufficient to describe the physical phenomena occurring in this material

Congress communications

ZEOLITE A / POLY(1-TRIMETHYLSILYL-1-PROPYNE MIXED MATRIX MEMBRANES FOR CO_2/N_2 SEPARATION
Fernández-Barquín, A; Casado-Coterillo, C.; Valencia, S.; Irabien, A.
Poster Flash Presentation. IX Ibero-American Congress on Membrane Science and Technology.

INFLUENCE OF TEMPERATURE IN HIGHLY PERMEABLE MEMBRANES FOR THE CO_2/N_2 SEPARATION
Fernández-Barquín, A; Casado-Coterillo, C.; Valencia, S.; Irabien, A.
Keynote. II International congress of Chemical Engineering of ANQUE.

STUDY OF THE EFFECT OF MORPHOLOGY OF HIGHLY PERMEABLE POLYMERS AND ACETATE-BASED IONIC LIQUID HYBRID MEMBRANES ON CO_2/N_2 SEPARATION
Fernández-Barquín, A.; Casado-Coterillo, C.; Irabien, A.
Oral communication. 10th International Congress on Membrane and Membrane Processes.

DEVELOPMENT OF HIGHLY PERMEABLE, SELECTIVE, ROBUST MEMBRANE MATERIALS FOR CO_2 SEPARATION
Fernández-Barquín, A.; Casado-Coterillo, C.; Valencia, S.; Irabien, A.
Keynote. 21st International Congress of Chemical and Process Engineering.

PURE SILICA ZEOLITE ITQ-29 / POLY(1-TRIMETHYLSILYL-1-PROPYNE MIXED MATRIX MEMBRANES FOR CO2/N2 SEPARATION
Fernández-Barquín, A.; Casado-Coterillo, C.; Valencia, S.; Irabien, A.
Sent communication. 13th Mediterranean Congress of Chemical Engineering

Departamento de Ingenierías Química y Biomolecular

Universidad de Cantabria (SPAIN)

DePRO group

Department of Chemical and Biomolecular Engineering

ETSIIyT, Avda. los Castros s/n

Santander, Cantabria. SPAIN

E-mail: irabienj@unican.es

✉: **fbarquina@unican.es**

Financial support from the Spanish Ministry of Economy and Competitiveness (MINECO) under project CTQ2012-31229 at the Universidad de Cantab gratefully acknowledged.

Máster en Ingeniería química: "Producción y Consumo Sostenible"

DEVELOPMENT OF HIGHLY PERMEABLE, SELECTIVE, ROBUST MEMBRANE MATERIALS FOR CO_2 SEPARATION

Author: Ana FernándezBarquín **Advisor: Clara Casado Coterillo**
Dpto. Ingenierías Química y Biomolecular. Universidad de Cantabria.
✉: ETSIIyT. Avda. de los Castros s/n 39005 Santander. SPAIN 🖷: fbarquina@unican.es

Scope

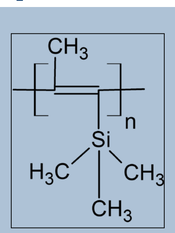

Figure 1. PTMSP

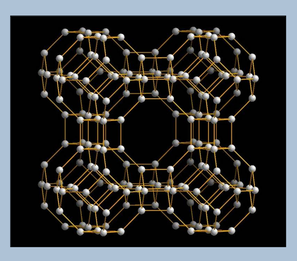

Figure 2. Zeolite LTA type

➢ Poly (1-trimethylsilyl-1-propyne) (PTMSP) (Fig. 1) has the highest known permeability of any polymer to gases. However, the high permeability is coupled with low selectivity.

➢ Zeolites are porous crystalline alumina-silicates composed of AlO_4 and SiO_2 tetrahedra. LTA type zeolites have pore dimensions of 0.4 nm, being able to discriminate between molecules as O_2 and N_2, is used in air separation (Fig. 2).

➢ Mixed matrix membranes (MMMs) of highly permeable and thermally resistant polymer, and small-pore Zeolite NaA (Si/Al=1) and Zeolite ITQ29 (Si/Al=∞) filler may provide robust, permeable and selective membranes for CO_2/N_2 separation.

Conclusions

✓ **MMMs have been prepared using highly permeable PTMSP and small pore LTA-type zeolites with different Si/Al ratio.**

✓ **Zeolites have increased the thermal stability of the membranes.**

✓ **The CO_2/N_2 selectivity has been improved by the addition of low loadings of small-pore zeolites, without compromising the high permeability of PTMSP.**

Experimental

Mixed matrix membranes preparation

PTMSP dissolution in toluente Refluxing at 60 ºC for 24 h + **Zeolite dispersion (5, 10 and 20 wt%) Stirring 2 h at ambient conditions**

↓

Solution casting method

↓

Evaporation Removal from glass plate Methanol treatment

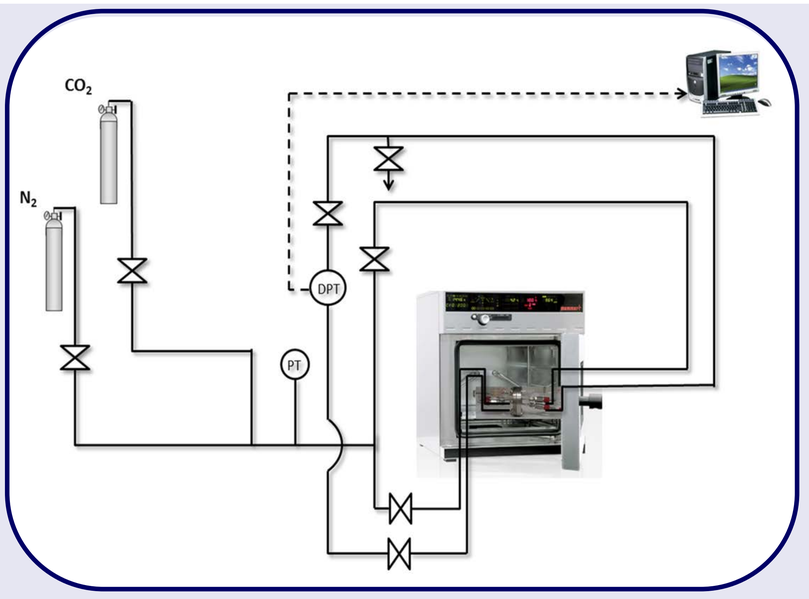

Figure 3. Experimental setup

Membrane characterization

X-ray difraction analysis

↓

45 kV and 40 mA
Cu Kα1 radiation (λ = 1.5406 Å)
Solid angle detector, step of 0.05º

↓

Gas permeation test

↓

25 – 100 ºC
2 – 3 bar

Thermogravimetrical analysis

CO_2 adsorption for 180 min at 25 – 60ºC
TGA in air at 10ºC/min up to 700 ºC

Results and discussion

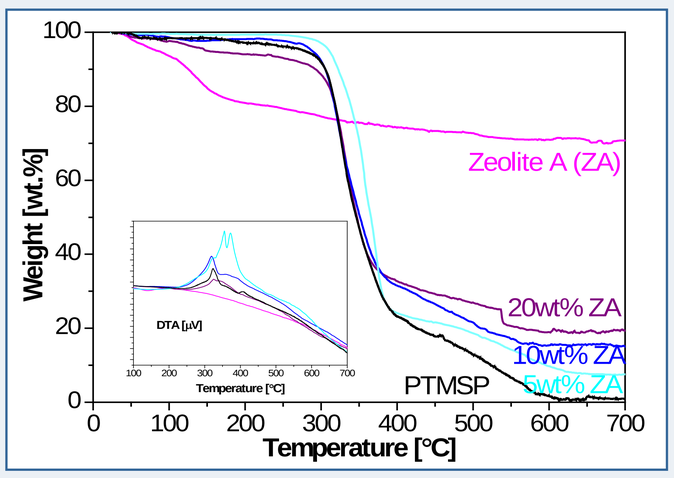

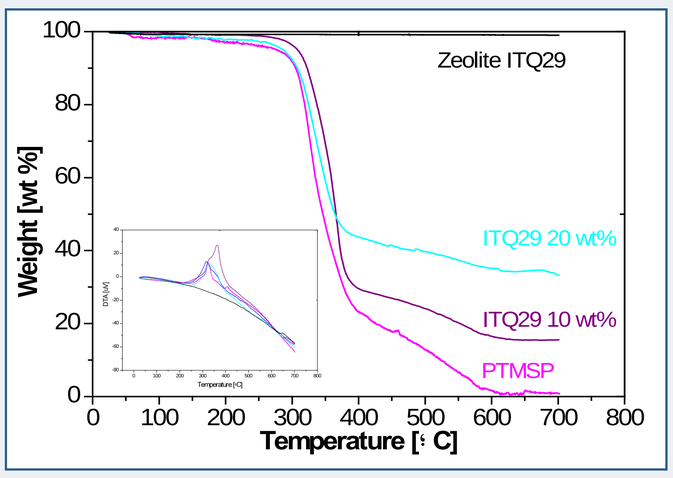

Figure 4. Thermogravimetric analyses

The real zeolite loading of PTMSP membranes obtained by TGA agreed with nominal value; the thermal stability of the membranes is similar to the glassy polymer PTMSP (Fig. 4)

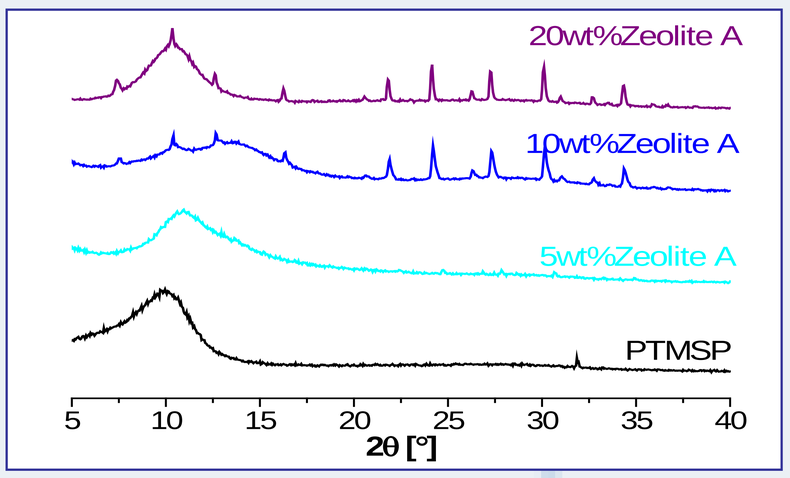

Figure 5. X-ray diffractograms

The X-ray diffraction (XRD) patterns of the films discern a good interaction between the zeolite and the polymer matrix (Fig.5)

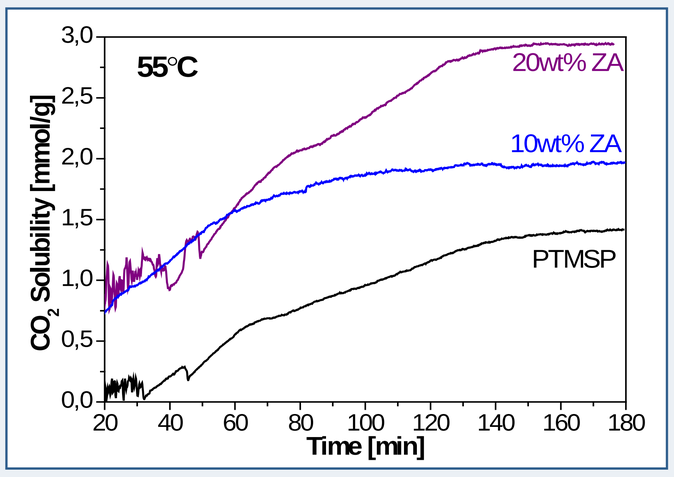

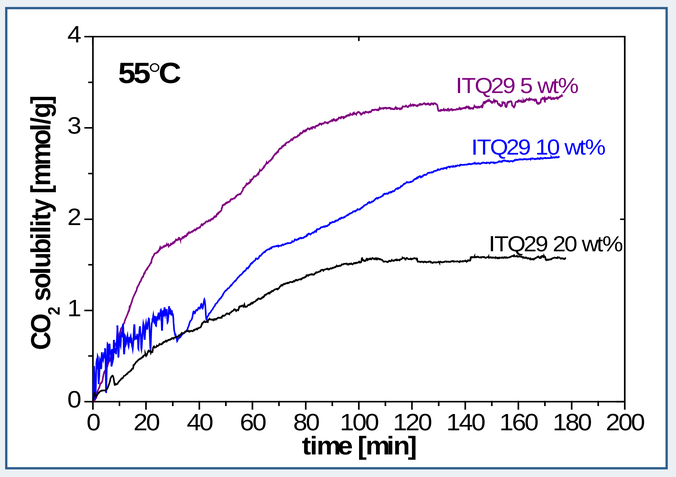

Figure 6. CO_2 adsorption curves at 55ºC

By filling PTMSP with zeolite A, the CO_2 loading increased as compared with the pure PTMSP membrane. With zeolite ITQ-29 as filler, CO_2 solubility decreases with loading of zeolite ITQ-29 (Fig. 6)

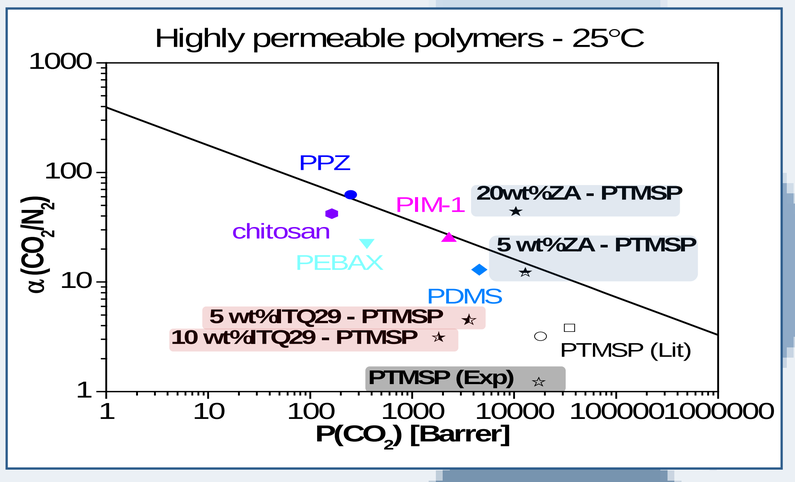

Figure 7. Robeson upperbound

Selectivity increases with zeolite loading without decreasing permeability, overcoming Robeson's upperbound (Fig.7)

References

[1] Robeson, L.M. 2008. *J. Membr. Sci.* 320. 390-400.
[2] Casado-Coterillo, C.; Soto, J.; Jimaré, M. T.; Valencia, S.; Corma, A.; Téllez, C.; Coronas, J. 2012. *Chem. Eng. Sci.* 73.116-122

Acknowledgements

Financial support from the Spanish Ministry of Economy and Competitiveness (MINECO) under project CTQ2012-31229 and Ramón y Cajal programme (RYC-2011-08550) at the University of Cantabria is gratefully acknowledged.